Applied Materials Today 9 (2017) 566–588

Contents lists available at ScienceDirect

Applied Materials Today

journal homepage: www.elsevier.com/locate/apmt

Review

Carbon nanotubes-based electrochemical (bio)sensors for biomarkers

Gustavo A. Rivas[a,*], Marcela C. Rodríguez[a], María D. Rubianes[a], Fabiana A. Gutierrez[a], Marcos Eguílaz[a], Pablo R. Dalmasso[b], Emiliano N. Primo[a], Cecilia Tettamanti[a], María L. Ramírez[a], Antonella Montemerlo[a], Pablo Gallay[a], Concepción Parrado[c]

[a] INFIQC, Departamento de Fisicoquímica, Facultad de Ciencias Químicas, Universidad Nacional de Córdoba, Ciudad Universitaria, 5000 Córdoba, Argentina
[b] CIQA, Departamento de Ingeniería Química, Facultad Regional Córdoba, Universidad Tecnológica Nacional, 5016 Córdoba, Argentina
[c] Departamento de Química Analítica, Facultad de Ciencias Químicas, Universidad Complutense de Madrid, 28040 Madrid, Spain

ARTICLE INFO

Article history:
Received 31 August 2017
Received in revised form 15 October 2017
Accepted 16 October 2017

Keywords:
Carbon nanotubes
Electrochemical (bio)sensors
Biomarkers

ABSTRACT

This review is focused on the critical discussion about the most representative carbon nanotubes (CNTs)-based electrochemical (bio)sensors for the quantification of different biomarkers of clinical relevance reported in the period 2013–2017 (carcynoembryonic antigen, prostate specific antigen, alpha-fetoprotein, cytokines, cardiac biomarkers, insulin growth factor-1, β-galactoside-α-2,6-sialyltransferase, DNA sequences, microRNAs, and dopamine). We concentrated our attention on the molecules used as (bio)recognition elements, the approaches for immobilizing these (bio)recognition molecules at the electrode surfaces, the strategies to generate the analytical signal (label-free or labeled), the analytical performance of the resulting (bio)sensors, and the role of CNTs in these different aspects.

Contents

* Corresponding author.
E-mail address: grivas@fcq.unc.edu.ar (G.A. Rivas).

https://doi.org/10.1016/j.apmt.2017.10.005
2352-9407/

1. Introduction

The advent of nanobiotechnology has changed the paradigms of biosensing due to the unique properties of nanomaterials [1–3]. In particular, after the first carbon nanotubes (CNTs)-based electrochemical sensor reported by Britto et al. [4], CNTs have received enormous attention for the development of electrochemical (bio)sensors [5–9]. CNTs are allotropes of carbon that consist of a graphene sheet rolled into a tube usually capped at both ends by one half of a fullerene-like molecule [10,11]. Single-walled carbon nanotubes (SWCNTs) consist of a graphene sheet rolled defining a cylinder of several microns long and 0.4–2 nm diameter while multi-walled carbon nanotubes (MWCNTs) are concentric and closed tubules with two or multiple layers of graphene separated by approximately 0.34 nm defining a diameter between 2 and 100 nm [12]. CNTs present several advantages mainly connected with their high surface-to-volume ratio, their exceptional electronic properties and the presence of edge-plane like defects that make them a very interesting material for the construction of electrochemical (bio)sensors [13–17] in addition to the multiple applications in many other fields that are out of the scope of this review and have been extensively reviewed. However, it is important to remark that, in spite of these excellent characteristics, CNTs must be functionalized either covalently or non-covalently to minimize the van der Waals forces and π–π stacking interactions between the tubes before using them for building electrochemical sensors [18–24].

Biomarkers are defined by the National Institute of Health as "a characteristic that is objectively measured and evaluated as an indicator of normal biological/pathogenic processes or pharmacological responses to a therapeutic intervention" [25]. They can be used for diagnosis, prognosis, risk assessment, evaluation of therapy effectiveness, and evolution of a disease; therefore, the detection of very low concentrations of biomarkers is extremely important. In this sense, electrochemical (bio)sensors represent an interesting alternative due to their multiple advantages connected with high sensitivity, high specificity, low cost, friendly operation, miniaturization, and portability [8,26,27].

The goal of this review is to present a comprehensive overview of the most representative CNTs-based electrochemical (bio)sensors for the quantification of biomarkers of clinical relevance covering the period from 2013 to June 2017. In the following sections, we critically discuss the nature of the (bio)recognition element, the preparation of the (bio)recognition layer, the strategy for transducing the (bio)affinity event, and the analytical performance of the resulting biosensors for the quantification of the different biomarkers.

2. Carbon nanotubes-based electrochemical (bio)sensors for protein biomarkers

2.1. Carcinoembryonic antigen

Carcinoembryonic antigen (CEA) belongs to the family of cell-surface glycoproteins [28]. It is a complex, highly glycosylated macromolecule with a molecular weight of 200 kDa, produced by cells of the gastrointestinal tract during embryonic development [29]. Since the concentration largely decreases after birth, the levels of CEA should be minimal in the blood of healthy adults (lower than 2.5 ng mL^{-1}) [30]. Elevated concentrations have been associated with ovarian carcinoma, breast and lung cancer [31], and especially colorectal adenocarcinoma [32]. Thus, CEA is one of the most widely used tumor biomarkers and its quantification is extremely useful for evaluating the success of a tumor surgery, the effectiveness of a cancer therapy, and the recovery prognosis. Different alternatives have been proposed for the quantification of CEA [33]. In this section, we discuss the most representative CNTs-based CEA electrochemical biosensors published between 2013 and 2017 with special emphasis on the critical comparison of the different bioanalytical platforms for the immobilization of anti-CEA primary antibody (Ab_1) and the different strategies for transducing the bioaffinity event. Table 1 summarizes the main characteristics of these biosensors.

Li et al. [34] reported an interesting alternative for the label-free electrochemical immunosensing of CEA based on the use of glassy carbon electrodes (GCE) modified with gold nanoparticles (AuNPs)-functionalized magnetic MWCNTs containing Pb(II) (Pb(II)@AuNPs@MWCNTs-Fe_3O_4) as platform for the immobilization of Ab_1 and for the catalytic reduction of hydrogen peroxide. The association of the different components presented several advantages connected to the increment of the surface area, that made possible the incorporation of higher amounts of Ab_1, and the synergism in the electrocatalysis toward the reduction of hydrogen peroxide, that allowed an important enhancement of the analytical signal. The immunosensor presented a wide linear relationship between H_2O_2 reduction current and log C_{CEA} (0.0005 pg mL^{-1} to 50 ng mL^{-1}), with a detection limit of 1.7 fg mL^{-1}. No appreciable interference was observed in the presence of human

Table 1
CNT-based electrochemical biosensors for carcinoembryonic antigen.

(Bio)sensor type	Platform	Label	Detection	Linear range	Detection limit	Sample	Ref.
Immunosensor	GCE/Pb(II)@AuNPs@MWCNTs-Fe_3O_4/Ab_1	Free	Amperometry	5 fg mL^{-1} to 50 ng mL^{-1}	1.7 fg mL^{-1}	Serum	[34]
Immunosensor	GCE/GO-cMWCNTs-AuNPs-CeO_2NPs-Chit/Ab_1	Free	ECL	0.05–100 ng mL^{-1}	0.02 ng mL^{-1}	Serum	[35]
Immunosensor	GCE/AuNPs-Thionine-CNTs/Ab_1	Ab_2-AuNPs-PANI-CNTs-HRP	DPV	0.02–3.0 ng mL^{-1}	0.008 ng mL^{-1}	Serum	[36]
Immunosensor	GCE/β-CD-MWCNTs/Ab_1	Ab_2-MWCNTs-MnO_2-AgNPs	Amperometry	0.0001–0.5 ng mL^{-1}	0.03 pg mL^{-1}	Serum	[37]
Immunosensor	GCE/β-CD-MWCNTs/ADA-Ab_1	Ab_2-FcCOOH-NH_2-β-CD@Fe_3O_4@SiO_2	SWV	0.001–15 ng mL^{-1}	0.33 pg mL^{-1}	—	[38]
Immunosensor	GCE/NH_2-Gr/Ab_1	Ab_2-NH_2-MWCNTs-PdPtNCs	Amperometry	0.001–20 ng mL^{-1}	0.2 pg mL^{-1}	Serum	[39]
Immunosensor	GCE/SnO_2-rGO-AuNPs/Ab_1	Ab_2-PdNPs-V_2O_5-MWCNTs	Amperometry	0.5 pg mL^{-1} to 25 ng mL^{-1}	0.17 pg mL^{-1}	Serum	[40]

Abbreviations: GCE: glassy carbon electrode; AuNPs: gold nanoparticles; MWCNTs: multi-walled carbon nanotubes; Ab_1: anti-CEA primary antibody; GO: graphene oxide; cMWCNTs: carboxylated multi-walled carbon nanotubes; CeO_2NPs: ceria nanoparticles; Chit: chitosan; Ab_2: anti-CEA secondary antibody; PANI: polyaniline; HRP: horseradish peroxidase; β-CD: β-cyclodextrin; AgNPs: silver nanoparticles; ADA: adamantine carboxylic acid; FcCOOH: ferrocene carboxylic acid; NH_2-Gr: amino graphene; PtPdNCs: PdPt nanocages; rGO: reduced graphene oxide; PdNPs: Pd nanoparticles.

G immunoglobin (IgG), alpha-fetoprotein (AFP), bovine serum albumin (BSA), glucose, and ascorbic acid. Pang et al. [35] reported another interesting label-free CEA immunosensor based on electrochemiluminescent (ECL) detection. They proposed a bioanalytical platform obtained by modification of GCE with graphene oxide (GO), carboxylated MWCNTs (cMWCNTs) and AuNPs functionalized with ceria nanoparticles (CeO_2NPs) dispersed in chitosan (Chit). The transduction of the biorecognition event was performed in the presence of $K_2S_2O_8$ from the decrease of the ECL originated after interaction with CEA, with a detection limit of 0.02 ng mL^{-1}. Although the detection limit was not very competitive compared to other biosensors, this immunosensor demonstrated to be stable, selective (no interference of prostatic specific antigen (PSA), BSA, and AFP), with potential application in serum samples (recoveries between 98.9 and 102.6%).

Another group of CNTs-based CEA electrochemical immunosensors relied on the use of an anti-CEA secondary antibody (Ab_2) conjugated with different labels to amplify the detection of the bioaffinity event. In the following paragraphs, we compare the most representative strategies for the sandwich-type immunosensing, with special emphasis on the characteristics of Ab_2-tags and the transduction of the immunosensing event. Feng et al. [36] reported the use of AuNPs and thionine-functionalized CNTs as platform for the attachment of Ab_1. The label was obtained by deposition of AuNPs at polyaniline (PANI)-modified CNTs followed by the immobilization of horseradish peroxidase (HRP) and Ab_2. AuNPs and CNTs were used to improve the charge transfer and allow the "communication" between the active site of HRP, the redox mediator and the base electrode while PANI was responsible for higher loadings of CNTs, AuNPs, and HRP. The analytical signal was obtained by differential pulse voltammetry (DPV) from the electrochemical response of thionine in the presence of hydrogen peroxide. The authors reported a linear range between 0.02 and 3.0 ng mL^{-1} and a detection limit of 0.008 ng mL^{-1}. Special mention deserves the strategy reported by Han et al. [37], which was focused on the use of host–guest interaction for the immobilization of Ab_1. They proposed a sandwich-type immunosensor using GCE modified with MWCNTs functionalized with β-cyclodextrin (β-CD) (β-CD-MWCNTs) as support for Ab_1. The sandwich assay was performed with MWCNTs modified with MnO_2 and silver nanoparticles (AgNPs) containing Ab_2. In this supramolecular architecture, β-CD-MWCNTs improved the conductivity of the platform and facilitate the anchoring of Ab_1. AgNPs-MWCNTs/MnO_2 not only supports Ab_2 but also allowed a large improvement in the analytical signal. In fact, AgNPs and MnO_2 presented an important catalytic effect on the reduction of hydrogen peroxide, largely contributing to the efficiency of the analytical performance: linear relationship from 0.0001 to 0.5 ng mL^{-1}, detection limit of 0.02 pg mL^{-1}, highly satisfactory recovery percentages in serum samples, and reproducibility of 4.2%. Using a similar scheme, Yan et al. [38] reported a very innovative sandwich-type immunosensor using a supramolecular architecture where both Ab_1 and Ab_2 were loaded through host–guest interactions. In this case, Ab_1 functionalized with adamantine carboxylic acid (ADA) was associated to β-CD-MWCNTs modified GCE through the host–guest association between β-CD and ADA bond to Ab_1. Ab_2 functionalized with ferrocene carboxylic acid (FcCOOH) was associated to the tag-bioconjugate through host–guest interaction with amino-β-CD@Fe_3O_4@SiO_2 (NH_2-β-CD@Fe_3O_4@SiO_2-FcCOOH-Ab_2). The analytical signal was obtained from the reduction of hydrogen peroxide catalyzed by Fe_3O_4. The authors reported a linear range comparable (0.001–15 ng mL^{-1}) and a detection limit higher (0.33 pg mL^{-1}) than those obtained for the sensor previously described, suggesting that the combination of MnO_2 and AgNPs was more efficient for the catalytic reduction of hydrogen peroxide.

Other interesting approaches were focused on the integration of CNTs to the label instead of to the primary platform. Li et al. [39] proposed a labeled assay of CEA using GCE modified with amino-graphene (NH_2-Gr) and Ab_1 *via* EDC/NHS chemistry, where Gr increased the surface area, improved the conductivity of the platform and worked as support for attaching Ab_1. The label was very original and relied on the use of Ab_2 bound to NH_2-MWCNTs modified with PdPt nanocages (PdPtNCs) (Fig. 1). The association of Pd and Pt made possible an excellent electrocatalytic activity toward the reduction of hydrogen peroxide, offering a simple, fast, and efficient analytical performance with characteristics comparable to those reported by Yan et al. [38]. Another sensor was obtained by dropping a dispersion of SnO_2/reduced graphene oxide (SnO_2/rGO) nanocomposite at GCE followed by the deposition of AuNPs at the resulting electrode [40]. SnO_2/rGO was used to increase the surface area and, consequently, the amount of AuNPs and Ab_1. The label was prepared by using PdNPs associated with V_2O_5-modified MWCNTs and Ab_2. The analytical signal was obtained from the catalytic reduction of hydrogen peroxide at −0.400 V, largely enhanced due to the synergic effect of MWCNTs, V_2O_5, and PdNPs. Under

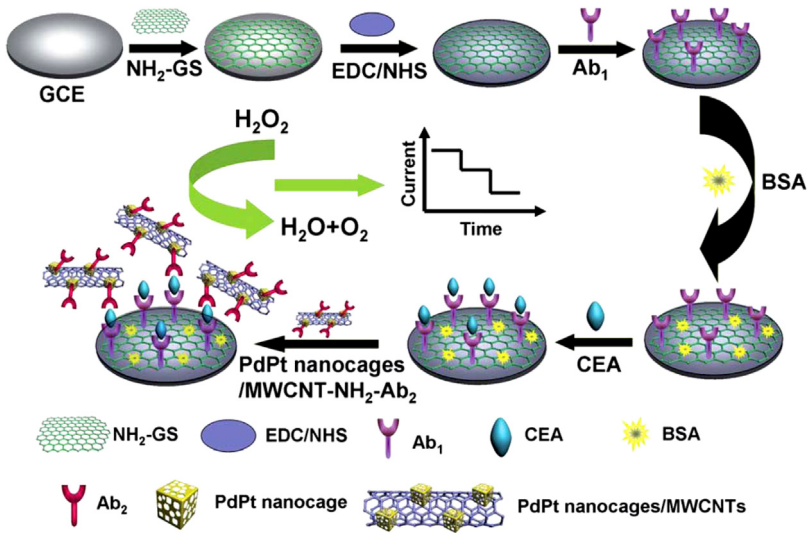

Fig. 1. Schematic illustration of the sandwich-type electrochemical immunosensor fabrication process for detection of CEA. Reproduced from Ref. [39] with permission of The Royal Society of Chemistry.

these conditions, the biosensor presented a linear range between 0.5 pg mL^{-1} and 25 ng mL^{-1} and a detection limit of 0.17 pg mL^{-1}, offering the widest linear range of the biosensors reported here and a detection limit comparable to previous reports. Recovery studies using serum samples demonstrated the potentiality of the proposed biosensor for further application in clinical analysis. The authors also evaluated the label-free response of the biosensor using only the primary platform (GCE/rGO-SnO_2/AuNPs/Ab_1); however, the analytical performance was not as good as for the labeled one, mainly due to a less efficient catalytic activity of the platform on the reduction of hydrogen peroxide.

2.2. Prostate specific antigen

Prostate specific antigen (PSA) is a protein of 240 amino acids and 34 kDa that belongs to the glandular kallikrein proteins family and it is currently considered the best serum marker for the detection of prostate cancer. The literature suggests that PSA values over 1.5 ng mL^{-1} should be used as a cut-off to consider further testing for all age groups and as a predictor of future risk of malignancy [41]. In this section, we present the most relevant strategies for PSA electrochemical (bio)sensing based on the use of CNTs either in the biorecognition platform or as label, involving bioaffinity (immunosensors and aptasensors) or affinity (molecularly imprinted polymers (MIP)-based sensors) interactions. Table 2 summarizes the most relevant characteristics of these platforms reported in the period covered by the review.

Peng et al. [42] developed a label-free immunosensor based on the layer-by-layer self-assembly of carboxylated MWCNTs (cMWCNTs), poly(dimethyldiallylammonium chloride) (PDDA), and ceria mesoporous nanospheres (CeO_2NSs) and the covalent immobilization of anti-PSA primary antibody (Ab_1). The transduction of the biorecognition event was performed by DPV through the decrease in the oxidation current of o-phenylenediamine (OPD) catalyzed by CeO_2NSs. The authors reported a very low detection limit (4 fg mL^{-1}) with a linear response from 0.01 to 1000 pg mL^{-1}. Kavosi et al. [43] proposed the use of a GCE modified with a composite made of MWCNTs, the ionic liquid 1-butyl-methylpyrrolidinium-bis(trifluoromethylsulfonyl)imide ([C4mpyr][NTf2]) and Chit (MWCNTs-[C4mpyr][NTf2]-Chit) as support for the subsequent immobilization of AuNPs decorated with polyamidoamine dendrimer (AuNPs-PAMAM), thionine, and Ab_1. The label-free PSA detection was performed by electrochemical impedance spectroscopy (EIS) using $[Fe(CN)_6]^{3-/4-}$ as redox indicator through the increase in the charge transfer resistance (R_{ct}) produced after PSA interaction.

Table 2
CNT-based electrochemical biosensors for prostate specific antigen.

(Bio)sensor type	Platform	Label	Detection	Linear range	Detection limit	Sample	Ref.
Immunosensor	GCE/cMWCNTs/PDDA/CeO_2NSs/Ab_1	Free	DPV	0.01–1000 pg mL^{-1}	4 fg mL^{-1}	Plasma	[42]
Immunosensor	GCE/MWCNTs-[C4mpyr][NTf2]-Chit/AuNPs-PAMAM/thionine/Ab_1	Free Ab_2-HRP	EIS DPV	EIS: up to 25 ng mL^{-1} DPV: 0.05–2 ng mL^{-1}	EIS: 0.5 ng mL^{-1} DPV: 1 pg mL^{-1}	Serum	[43]
Immunosensor	GCE/MWCNTs-[C4mpyr][NTf2]/thionine/Ab_1	Ab_2-HRP	DPV	0.2–1 ng mL^{-1}	20 pg mL^{-1}	Serum and biopsies	[44]
Immunosensor	GCE/MWCNTs/Ab_1	Ab_2-AuNPs-Fc	DPV	0.01–100 ng mL^{-1}	5.4 pg mL^{-1}	Serum	[45]
Immunosensor	GCE/cMWCNTs/Ab_1	Ab_2-AuNPs	LSV	0.18 fg mL^{-1} to 450 ng mL^{-1}	0.1 fg mL^{-1}	Serum	[46]
Immunosensor	GCE/MWCNTs-Naf/$(Ru(bpy)_3^{2+})$/Ab_1	Ab_2-pDA-NSs	ECL	0.1 pg mL^{-1} to 20 ng mL^{-1}	35 fg mL^{-1}	Serum	[47]
Immunosensor	GCE/MWCNTs-pDA-AuNPs/Ab_1	Ab_2-PAMAM-A_1/A_1-His/A_2-$Ru(dcbpy)_3^{2+}$	ECL	0.01 pg mL^{-1} to 40 ng mL^{-1}	4.2 fg mL^{-1}	Serum	[48]
Immunosensor	SPE/PtNPs-AuNPs/Ab_1	Ab_2-ZnOQDs-MWCNTs	ECL	1 pg mL^{-1} to 500 ng mL^{-1}	0.61 pg mL^{-1}	Serum	[49]
Immunosensor	GCE/rGO-AuNPs/Ab_1	Ab_2-rGO-MWCNTs-PdNPs	Amperometry	0.0005–15 ng mL^{-1}	0.17 pg mL^{-1}	Serum	[50]
Immunosensor	GCE/AuNPs/Ab_1	Ab_2-MWCNTs-PdAgHDs	Amperometry	0.0001–30 ng mL^{-1}	0.03 pg mL^{-1}	Serum	[51]
Immunosensor	GCE/AuNPs/Ab_1	Ab_2-NiCoBP-MWCNTs	DPV	0.1–50 ng mL^{-1}	0.035 ng mL^{-1}	Serum	[52]
Peptide sensor	GCE/MWCNTs-PAMAM/peptide/DSP-AuNPs-SiO_2/AgNPs	Free	LSV	0.001–30 ng mL^{-1}	0.7 pg mL^{-1}	Serum	[53]
Peptide sensor	GCE/MWCNTs-PAMAM-AuNPs/GA/peptide-AuNRs	Free	ECL	0.1 pg mL^{-1} to 10 ng mL^{-1}	30 fg mL^{-1}	Serum	[54]
Aptasensor	GCE/MWCNTs-Chit/GA/S_1-S_2/MB	Free	DPV	0.85–12.5 ng mL^{-1}	0.75 ng mL^{-1}	Serum	[55]
Aptasensor	GCE/MWCNTs-ERGO/AuNPs/Aptamer	Free	DPV EIS	DPV: 0.005–20 ng mL^{-1} EIS: 0.005–100 ng mL^{-1}	DPV: 1 pg mL^{-1} EIS: 1 pg mL^{-1}	Serum	[56]
MIPsensor	PGE/MWCNTs-MnNPs/MIP	Free	SWV DPV	SWV: 0.99 fg mL^{-1} to 5.99 pg mL^{-1} DPV: 9.99 fg mL^{-1} to 9.99 pg mL^{-1}	SWV: 0.25 fg mL^{-1} DPV: 3.04 fg mL^{-1}	Serum, urine, and forensic samples	[57]

Abbreviations: GCE: glassy carbon electrode; cMWCNTs: carboxylated multi-walled carbon nanotubes; PDDA: poly(diallyldimethylammonium chloride); CeO_2NSs: ceria mesoporous nanospheres; Ab_1: anti-PSA primary antibody; DPV: differential pulse voltammetry; MWCNTs: multi-walled carbon nanotubes; [C4mpyr][NTf2]: 1-butyl-methylpyrrolidinium-bis(trifluoromethylsulfonyl)imide ionic liquid; Chit: chitosan; AuNPs: gold nanoparticles; PAMAM: poly(amidoamine) dendrimer; Ab_2: anti-PSA secondary antibody; HRP: horseradish peroxidase; EIS: electrochemical impedance spectroscopy; Fc: ferrocene; LSV: linear sweep voltammetry; Naf: nafion; pDA-NSs: poly(dopamine) nanospheres; ECL: electrochemiluminescence; pDA: poly(dopamine); A_1: auxiliary DNA probe 1; His: histidine; A_2: auxiliary DNA probe 2; SPE: screen-printed electrode; PtNPs: platinum nanoparticles; ZnOQDs: ZnO quantum dots; rGO: reduced graphene oxide; PdNPs: palladium nanoparticles; PdAgHDs: palladium-silver heterodimers; DSP: dithiobis(succinimidylpropionate); SiO_2: SiO_2 particles; AgNPs: silver nanoparticles; GA: glutaraldehyde; AuNRs: gold nanorods; S_1: ssDNA capture probe; S_2: PSA-aptamer probe; MB: methylene blue; ERGO: electrochemically-reduced graphene oxide; PGE: pencil graphite electrode; MnNPs: manganese nanoparticles; MIP: molecular imprinted polymer.

The strategies based on the use of an amplification step involving a labeled anti-PSA secondary antibody (Ab_2) demonstrated to be very competitive. Kavosi et al. [43] reported the use of the biorecognition platform previously described (GCE/MWCNTs-[C4mpyr][NTf2]-Chit/AuNPs-PAMAM/thionine/Ab_1) associated to Ab_2 labeled with HRP. In this case, the analytical signal was obtained from the DPV peak current of thionine in the presence of hydrogen peroxide. The authors reported wider linear range and lower detection limit (pg mL^{-1} level) than in the case of the label-free impedimetric approach previously described, due to the catalytic activity of AuNPs toward thionine. Moreover, the proposed immunosensor was successfully used for PSA detection in serum samples with excellent precision and accuracy. The same group proposed another sandwich-type immunosensing strategy based on identical Ab_2-tag and MWCNTs-[C4mpyr][NTf2]/thionine/Ab_1 as biorecognition platform [44]. However, in this case the analytical performance was poorer due to the absence of AuNPs, responsible for the catalytic activity toward the reduction of hydrogen peroxide, and PAMAM, responsible for the efficient immobilization of the biorecognition element. It is important to remark that the proposed biosensor allowed the quantification of PSA not only in serum samples but also in biopsies. Yang et al. [45] reported an Ab_2 labeled with AuNPs and ferrocene (Fc) to develop a sandwich-type immunosensor using MWCNTs-modified GCE as platform for attaching Ab_1. The DPV signal of the anchored Fc allowed the quantification of PSA between 0.01 and 100 ng mL^{-1}, with a detection limit of 5.4 pg mL^{-1}. Qin et al. [46] developed an approach based on an ultrasensitive sandwich-type immuno-interface using cMWCNTs-modified GCE as support for the covalent immobilization of Ab_1 *via* EDC/NHS chemistry and Ab_2 labeled with gold-stained AuNPs. The analytical signal was obtained by anodic stripping voltammetry after the simultaneous chemical dissolution and cathodic preconcentration of the gold present in the supramolecular architecture. The analytical performance of this PSA biosensor was the best among the CNTs-based PSA electrochemical (bio)sensors reported in the period covered by this review, showing the lowest detection limit (0.1 fg mL^{-1}) and the widest linear range (from 0.18 fg mL^{-1} to 450 ng mL^{-1}). Liu et al. [47] developed a sandwich-type ECL immunosensor based on the use of Ab_1 immobilized at GCE modified with MWCNTs and $Ru(bpy)_3^{2+}$ and Ab_2 labeled with poly(dopamine) nanospheres (pDA-NSs). The efficient quenching ability of pDA-NSs allowed the authors to obtain a very good analytical performance, with a linear range from 0.1 pg mL^{-1} to 20 ng mL^{-1} and a detection limit of 35 fg mL^{-1}. Another CNTs-based PSA immunosensor relied on the use of a GCE modified with MWCNTs, AuNPs, and poly(dopamine) (pDA) as platform for the immobilization of Ab_1 [48]. The Ab_2 bioconjugate involved a PAMAM dendrimer to immobilize a super-sandwich DNA structure, $Ru(dcbpy)_3^{2+}$, and histidine to greatly amplify the ECL signal. The authors reported a very competitive detection limit (4.2 fg mL^{-1}) and a linear range between 0.01 pg mL^{-1} and 40 ng mL^{-1} with successful application in spiked normal human serum samples.

CNTs have also been used as label of Ab_2. As example, Liu et al. [49] presented an Ab_2 label constituted by MWCNTs and ZnO quantum dots (ZnOQDs). The biorecognition platform was built at screen printed electrodes (SPE) modified with AuNPs and platinum nanoparticles (PtNPs) used as support for the immobilization of Ab_1. This platform allowed the ECL detection of PSA in a wide linear range (from 1 pg mL^{-1} to 500 ng mL^{-1}) with a detection limit of 0.61 pg mL^{-1}. Tian et al. [50] reported a sandwich-type immunosensor obtained by modification of GCE with rGO, AuNPs, and Ab_1, using Ab_2 labeled with MWCNTs, rGO, and palladium nanoparticles (PdNPs) (rGO-MWCNTs-PdNPs) as amplification layer. The nanohybdrid rGO-MWCNTs-PdNPs exhibited high electrocatalytic activity toward the reduction of H_2O_2 largely amplifying the signal of the immunosensor. The bioplatform allowed the amperometric quantification of PSA at sub-pg mL^{-1} level. More recently, the same group [51] presented a sandwich-type immunosensor based on the use of a GCE modified with AuNPs as support for the immobilization of Ab_1 and Ab_2 labeled with a nanohybrid of MWCNTs and Pd-Ag heterodimers (PdAgHDs). The amperometric detection of H_2O_2 led to a competitive detection limit (0.03 pg mL^{-1}) and a linear range broader than the previous one [50]. Zhang et al. [52] developed a sandwich-type immunosensor based on GCE modified with AuNPs as support for Ab_1 immobilization and Ab_2 labeled with NiCoBP-MWCNTs *via* carbodiimide coupling method. The analytical signal was obtained by DPV from the catalytic oxidation of glucose in the presence of NiCoBP nanoparticles. The preparation of this sensor was relatively simple although the analytical performance was not as good as the previous ones, indicating the importance of the catalyst selected for labeling Ab_2.

In addition to the successful immunosensing of PSA, affinity biosensors based on the use of PSA specific peptides have been also reported. In a very innovative approach, He et al. [53] proposed the use of the peptide CEHSSKLQLAK-NH_2 for the biorecognition of PSA. The scheme for the different steps during the preparation of the biosensor is shown in Fig. 2. The peptide was attached to the surface of a MWCNTs-PAMAM modified GCE (GCE/MWCNTs-PAMAM) *via* cross-linking with N-succimnimidyl-3-(2-pyridyldithiol)propionate (SPDP). Subsequently, the dithiobis(succinimidylpropionate)(DSP)-AuNPs-SiO_2 conjugate, used as tracing tag, was covalently bond to the peptide *via* the interaction between DSP and the amino group of the peptide. Once the recognition PSA-peptide occurred, the peptide was specifically cleaved resulting in the loss of the tracing tag. Further *in situ* deposition of silver on the remaining DSP-AuNPs-SiO_2 nanohybrids made possible the sensitivity quantification of PSA, with a linear range between 0.001 and 30 ng mL^{-1} and a detection limit of 0.7 pg mL^{-1}. The biosensor showed satisfactory recoveries in human blood serum samples spiked with different concentrations of PSA. Wu et al. [54] reported an ECL biosensor based on resonance energy transfer (RET) for detecting PSA using $[Ru(bpy)_3]^{2+}$. The platform constituted by a film of MWCNTs, PAMAM, and AuNPs, offered a very active surface for the charge transfer and a high density of amine groups for the immobilization of the specific peptide CHSSKLQK labeled with gold nanorods (AuNRs). The peptide worked as ECL-RET acceptor due to the excellent overlap between the ECL emission spectrum of $[Ru(bpy)_3]^{2+}$ and the absorption spectrum of AuNRs, producing a decrease of the ECL signal. The interaction of the peptide with PSA produced the cleavage of the peptide and the release of AuNRs-peptide, allowing the recovery of the ECL signal. Using this approach, the detection limit was 30 fg mL^{-1} demonstrating an interesting improvement compared to the PSA-peptide based biosensor described by He et al. [53].

In addition to the interesting immunosensing and peptide-based strategies previously discussed, innovative approaches based on aptamers (the so-called "chemical antibodies") as PSA biorecognition elements have been also proposed. For example, Tahmasebi and Noorbakhsh [55] prepared a label-free aptasensor for PSA quantification based on the use of MWCNTs modified with Chit for the covalent attachment of ssDNA probe (S_1) as capture element of the PSA-aptamer (S_2). The analytical signal was obtained from the response of the redox indicator methylene blue (MB) originated from the preferential affinity of MB to S_1, compared to the hybrid probe/aptamer (S_1-S_2), and the higher affinity of the aptamer toward PSA, compared to its complementary DNA sequence. As a result of this play of affinities, the response for MB increased with the concentration of PSA, showing a linear range from 0.85 to 12.5 ng mL^{-1} and a detection limit of 0.75 ng mL^{-1}.

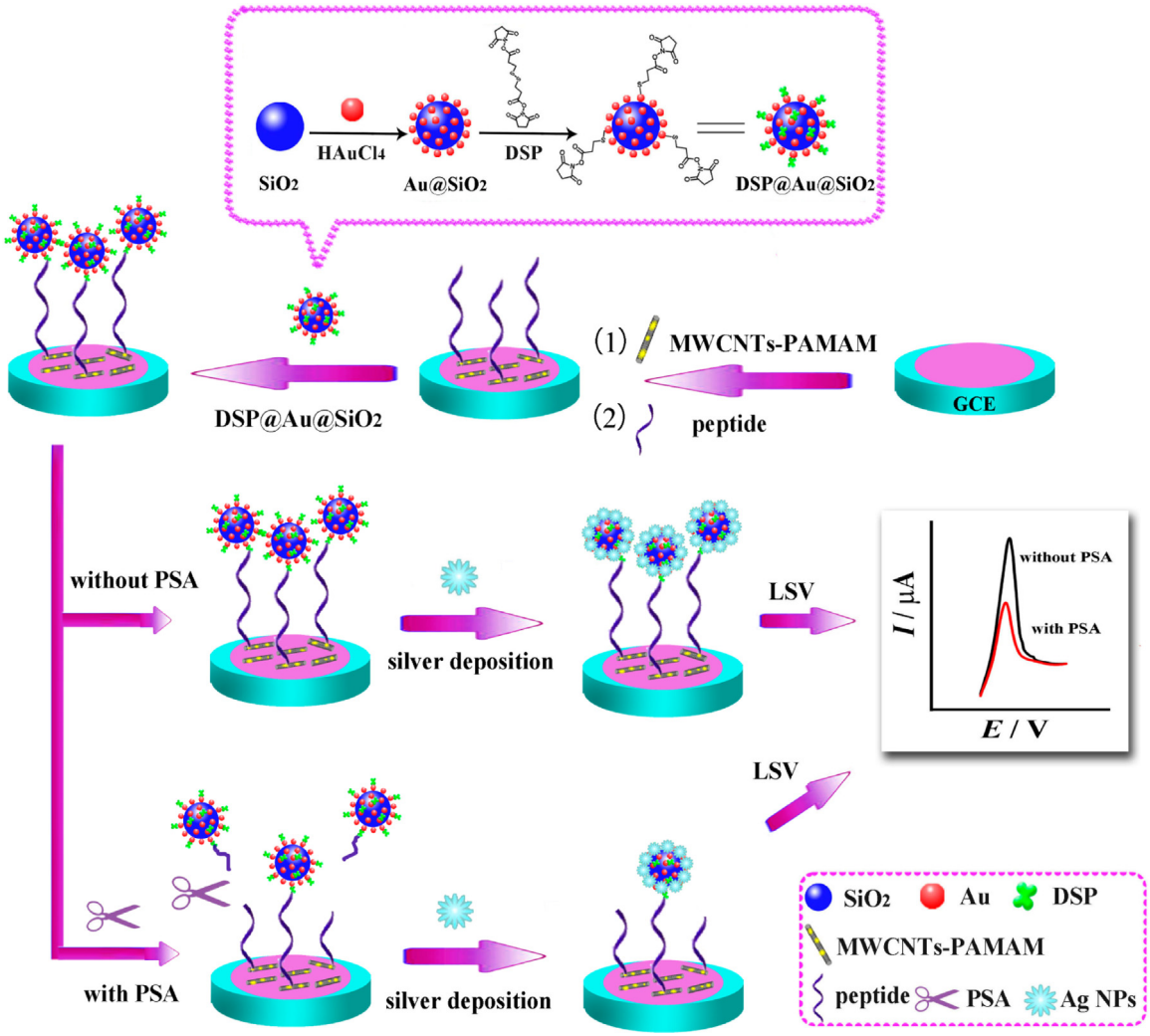

Fig. 2. Schematic diagram of the electrochemical-peptide biosensor fabrication process for detection of PSA.
Reprinted from Ref. [53]. Copyright 2015 American Chemical Society.

Heydari-Bafrooei and Shemszadeh [56] prepared a label-free PSA-aptasensor that relied on the use of a GCE modified with an electrochemically reduced GO (ERGO), MWCNTs, and AuNPs for the immobilization of the anti-PSA aptamer. The detection was based on the variation of charge transfer resistance (R_{ct}) (by EIS) and peak currents (by DPV) using $[Fe(CN)_6]^{3-/4-}$ as redox marker. The association of ERGO, MWCNTs, and AuNPs allowed an important improvement in the analytical characteristics of the biosensor with linear ranges from 0.005 to 20 ng mL^{-1} and 0.005 to 100 ng mL^{-1} for DPV and EIS, respectively, and detection limits of 1 pg mL^{-1} in both cases. Even when these aptasensors do not represent an improvement in the analytical performance, they offer an interesting alternative for building PSA biosensors due to the known advantages of aptamers compared to antibodies.

Finally, it is important to describe another strategy for PSA quantification focused on the use of CNTs as a support matrix for the preparation of MIPs. Patra et al. [57] described a PSA sensor with a very interesting transduction of the recognition event through the use of a three-dimensional MIP matrix synthesized at a pencil graphite electrode (PGE) modified with MWCNTs decorated with MnO_2 nanoparticles (MnO_2NPs) functionalized with thio-group to make a nano-iniferter. This nano-iniferter was used as platform to synthesize the MIP by a controlled radical polymerization technique using PSA as template. The binding sites in the outer layer of the polymer grafted over the CNTs improved the accessibility of the antigen and allowed the construction of a label-free sensor for the detection of PSA based on the direct reduction of the disulfur bonds of the captured PSA. The detection limits were 0.25 pg mL^{-1} and 3.04 pg mL^{-1} by SWV and DPV, respectively. The proposed sensor demonstrated an excellent selectivity and it was successfully used for PSA detection in human blood serum, urine, and forensic samples without any cross-reactivity, at the same time that offered a very particular transduction of the biorecognition event without involving additional reagents or labels.

2.3. Alpha-fetoprotein

Alpha-fetoprotein (AFP) is a plasma oncofetal glycoprotein with a molecular weight of approximately 70 kDa mainly produced by liver, yolk sac, and gastrointestinal tract of human fetus [58–60]. It is genetically and structurally related to albumin and it presents physicochemical properties similar to this protein. In fact, in the embryo, AFP has a biological role similar to the one of albumin in the adult [61]. The average concentration in healthy adults is around 3.4 ng mL^{-1} while the newborns present higher levels of AFP up to the first year of life. In pregnant women, AFP is an important marker for the detection of neural tube and ventral wall defects. Elevated levels of AFP have been found in patients with hepatocellular

Table 3
CNT-based electrochemical biosensors for alpha-fetoprotein.

(Bio)sensor type	Platform	Label	Detection	Linear range	Detection limit	Sample	Ref.
Immunosensor	SPE/cSWCNTs/WGA-Ab_1	—	EIS	0.001–0.1 ng mL^{-1}	1×10^{-4} ng mL^{-1}	Serum	[68]
Immunosensor	cSWCNTs/TMCS-MPS-Ab_1	—	DPV	0.1–100 ng mL^{-1}	0.06 ng mL^{-1}	—	[69]
Immunosensor	GCE/PB/SWCNTs-PLL/HRP-Ab_1	—	DPV	0.05–10.0 ng mL^{-1}	0.011 ng mL^{-1}	Serum	[70]
Immunosensor	GCE/MWCNTs-β-CD-FcCOOH-Ab_1	Ab_2-ADA-β-CD-AgNPs-GOx-ADA	SWV	0.001–5.0 ng mL^{-1}	0.2 pg mL^{-1}	Serum	[64]
Immunosensor	GCE/pDA-N-MWCNTs-Ab_1	Ab_2-Au@Pt-NH_2-Gr	Amperometry	0.1 pg mL^{-1} to 10 ng mL^{-1}	0.05 pg mL^{-1}	—	[71]
Immunosensor	GCE/MWCNTs/AuNRs/Ab_1	Ab_2-AuNRs-HRP	DPV	0.1–100 ng mL^{-1}	30 pg mL^{-1}	Serum	[62]
Immunosensor	GCE/cMWCNTs-Ab_1	Ab_2-Fe_3O_4@C@Pd	Amperometry	0.5 pg mL^{-1} to 10 ng mL^{-1}	0.16 pg mL^{-1}	Serum	[72]
Immunosensor	GCE/AuNPs-Ab_1	Ab_2-Fe_3O_4-MWCNTs@Au@Pb(II)	Amperometry	10 fg mL^{-1} to 100 ng mL^{-1}	3.33 fg mL^{-1}	Serum	[73]
Immunosensor	GCE/Gr-β-CD-Ab_1	Ab_2-MWCNTs-Pt@CuO	Amperometry CV	1 pg mL^{-1} to 20 ng mL^{-1}	0.33 pg mL^{-1}	Serum	[74]
Immunosensor	GCE/AuNPs-MPTS-Ab_1	Ab_2-thionine-HRP/AuNPs-PDDA-MWCNTs	DPV	0.01–50 ng mL^{-1}	3 pg mL^{-1}	Serum	[75]
Immunosensor	AuE/AuNPs-Ab_1	Ab_2-MWCNTs-PDDA-AuNPs-Pb(II)	SWV	0.01–60 ng mL^{-1}	4.5 pg mL^{-1}	Serum	[76]
Immunosensor	GCE/nano-Au film-Ab_1	Ab_2-cMWCNTs-PdNPs-GOx&HRP	ECL	up to 100 ng mL^{-1}	3.3 fg mL^{-1}	Serum	[77]
Immunosensor	GCE/CNTs@PNFs/Chit-Ab_1	—	ECL	0.1 pg mL^{-1} to 160 ng mL^{-1}	0.09 pg mL^{-1}	—	[78]

Abbreviations: AFP: alpha-fetoprotein; SPE: screen-printed carbon electrode; cSWCNTs: carboxylated single-walled carbon nanotubes; WGA: wheat-germ agglutinin lectin; Ab_1: anti-AFP primary antibody; EIS: electrochemical impedance spectroscopy; TMCS: trimethylchlorosilane; MPS: mesoporous silica; DPV: differential pulse voltammetry; GCE: glassy carbon electrode; PB: Prussian blue; SWCNTs: single-walled carbon nanotubes; PLL: polylysine; HRP: horseradish peroxidase; β-CD: cyclodextrin; FcCOOH: ferrocene carboxylic acid; Ab_2: anti-AFP secondary antibody; ADA: adamantine carboxylic acid; GOx: glucose oxidase; AgNPs: silver nanoparticles; pDA: poly(dopamine); N-MWCNTs: N-doped multi-walled carbon nanotubes; NH_2-Gr: amino-graphene; AuNRs: gold nanorods; cMWCNTs: carboxylated multi-walled carbon nanotubes; AuNPs: gold nanoparticles; MPTS: 3-mercaptopropyl trimethoxysilane; PDDA: poly(diallyldimethylammonium chloride); AuE: gold electrode; CV: cyclic voltammetry; PdNPs: palladium nanoparticles; SWV: square wave voltammetry; PNFs: nanofiber; Chi: chitosan, ECL: electrochemiluminescence.

carcinoma (HCC) and yolk sac-derived germ cell tumors, benign liver diseases (hepatitis and cirrhosis), and less frequently in patients with other tumors [61–63]. AFP is an important biomarker for the early diagnosis and monitoring of HCC and it is widely used for monitoring anti-neoplastic drug therapy in patients with HCC or germinal neoplasm [60,61]. Several methods have been developed for the detection of AFP [59,64–66]; among them, electrochemical biosensors have received enormous attention in the last years due to their known advantages [58,63,67]. Table 3 summarizes the analytical characteristics of recent CNTs-based electrochemical biosensors for the quantification of AFP, either label-free or labeled with different tags.

Yang et al. [68] developed a label-free glycobiosensor obtained by covalent immobilization of wheat-germ agglutinin (WGA) lectin at SPE modified with carboxylated SWCNTs (cSWCNTs). The increase in R_{ct} with the amount of AFP was used as analytical signal. The detection limit was 0.1 ng mL^{-1} and the linear range, 1–100 ng mL^{-1}. The lectin-based biosensor was also used to evaluate the glycan expression of AFP (AFP N-glycan) in serum samples to discriminate between healthy and cancer patients. Lin et al. [69] proposed a sensitive label-free detection of AFP using a biosensor prepared by covalent attachment of cSWCNTs and anti-AFP primary antibody (Ab_1) inside the channels of mesoporous silica (MSP) previously grafted with aminopropylethoxysilane. The conjugate anti-AFP/cSWCNTs/TMCS–MPS (where trimethylchlorosilane (TMCS) was used to block the external silanol groups of MSP) and Gr were immobilized at the electrode surface through a layer-by-layer self-assembly using polyvinyl alcohol as binding agent. The electrochemical response of the redox mediator FcCOOH, that was improved by the CNTs located inside the porous and the Gr present at the electrode surface, was used as analytical signal through the changes produced by the blocking effect of AFP. This immunosensor presented a detection limit of 0.06 ng mL^{-1} and a linear range from 0.1 to 100 ng mL^{-1}. Wang et al. [70] reported a label-free AFP inmunosensor based on a Prussian blue (PB) film-modified GCE coated with SWCNTs functionalized with polylysine (PLL-SWCNTs) as a biocompatible platform to immobilize Ab_1 modified with HRP. The catalytic current of H_2O_2 obtained by DPV was linearly related to AFP concentration in the range of 0.05–10.0 ng mL^{-1} with a detection limit of 0.011 ng mL^{-1}. The immunosensor was successfully used for the determination of AFP in human blood plasma.

Regarding the sandwich-type immunosensors, several strategies have been reported for the quantification of AFP. Gao et al. [64] proposed a very innovative approach based on host–guest interaction. Fig. 3 displays the different steps followed during the preparation of the biosensor. A GCE modified with MWCNTs functionalized with β-CD and FcCOOH was used for the covalent attachment of Ab_1. Ab_2 labeled with ADA was attached to glucose oxidase (GOx)-β-CD-functionalized AgNPs and the resulting conjugate transformed glucose into gluconic acid, generating hydrogen peroxide, which was catalytically reduced by AgNPs, highly improving the oxidation of FcCOOH. The fabricated immunosensor was very competitive, exhibiting high sensitivity, a linear range from 0.001 to 5.0 ng mL^{-1} and detection of sub-pg mL^{-1} levels (detection limit of 0.2 pg mL^{-1}). Jiao et al. [71] reported a dual enhancing sandwich-type electrochemical immunosensor using a GCE modified with N-doped MWCNTs (N-MWCNTs) functionalized with pDA as support for the immobilization of Ab_1. The transduction of the signal was performed using Ab_2 labeled with NH_2-Gr loaded with mesoporous Au@Pt nanodendrites. The electrocatalytic reduction of hydrogen peroxide at this surface was used as analytical signal. This relatively simple strategy allowed the authors to obtain a very competitive detection limit (0.05 pg mL^{-1}). Guo et al. [62] proposed an immunosensor obtained by assembling CNTs and AuNRs for the immobilization of Ab_1, using Ab_2 labeled with HRP-functionalized AuNRs nanocomposites (HRP-AuNRs) for the immunodetection of PSA. The analytical signal was obtained by DPV using H_2O_2 as substrate and 3,3′,5,5′-tetramethylbenzidine (TMB) as redox mediator. There was a linear response between 0.1 and 100 ng mL^{-1} with a detection limit of 30 pg mL^{-1}. Ji et al. [72] proposed a biorecognition platform prepared by immobilization of Ab_1 at GCE modified with cMWCNT,

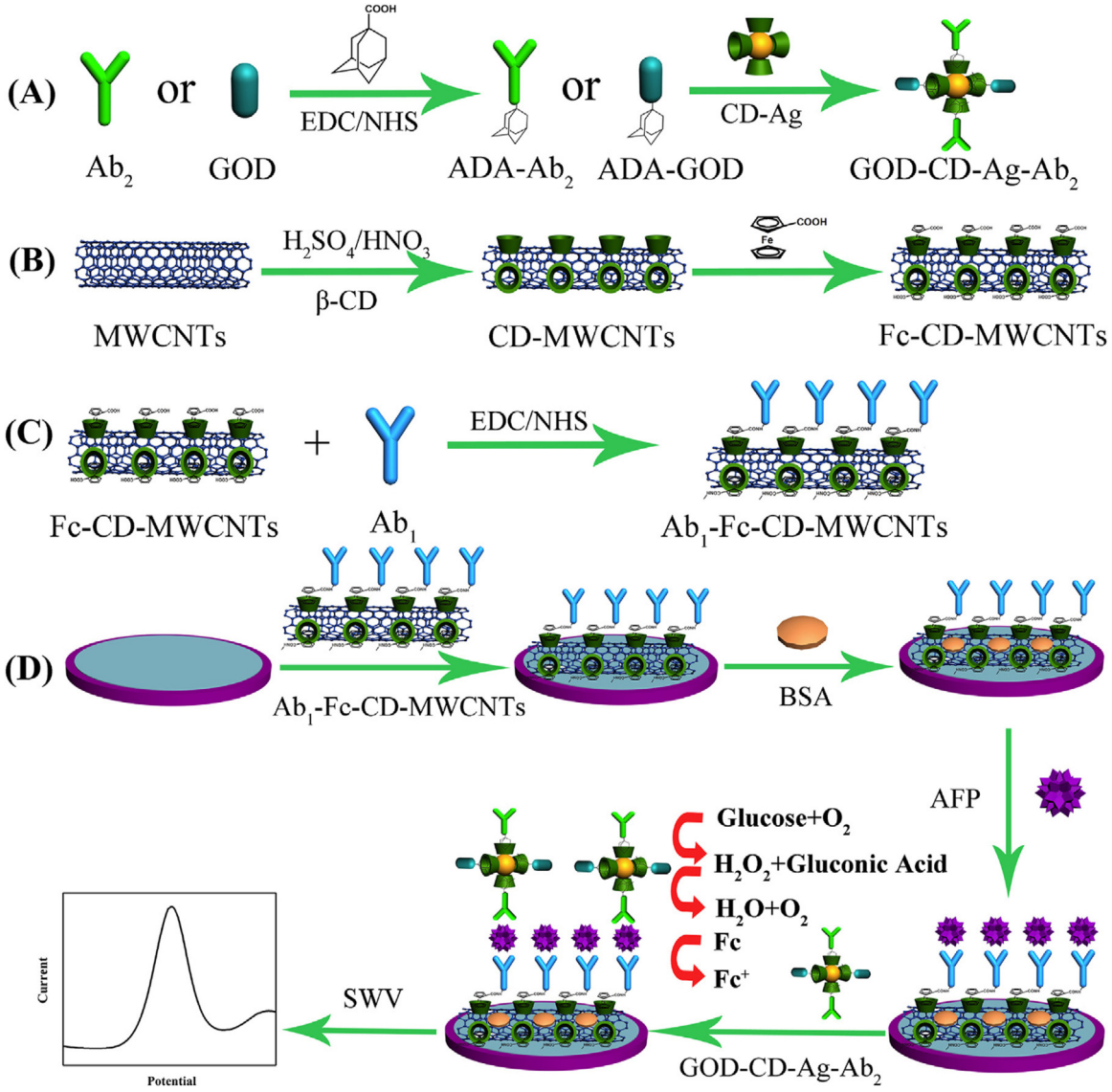

Fig. 3. Schematic illustration of the electrochemical immunosensor fabrication process for detection of AFP.
Reprinted from Ref. [64], Copyright (2015), with permission from Elsevier.

using a core-shell Fe_3O_4@C@Pd nanocomposite as label for Ab_2. The amperometric detection of H_2O_2 largely improved due to the presence of Pd nanoparticles, allowing to reach a detection limit of 0.16 pg mL^{-1} and a linear range from 0.5 pg mL^{-1} to 10 ng mL^{-1} with good selectivity, reproducibility, and stability.

CNTs have also been used as labels of Ab_2. Li et al. [73] reported a sandwich-type electrochemical immunosensor that allowed to obtain the lowest detection limit from the CNTs-based AFP electrochemical (bio)sensors published between 2013 and 2017. The strategy was based on the immobilization of Ab_1 at GCE modified by electrodeposition of AuNPs, and the use of (Pb(II)@Au@MWCNTs-Fe_3O_4) nanocomposite as label for Ab_2. The association of the different components of this nanocomposite demonstrated a synergic effect on the electrocatalytic activity toward the reduction of H_2O_2 giving a linear range between 10 fg mL^{-1} and 100 ng mL^{-1} and a detection limit of 3.33 fg mL^{-1}. Jiang et al. [74] designed a sandwich-type electrochemical immunosensor for AFP, using β-CD functionalized Gr (Gr-β-CD) to capture efficiently Ab_1. Pt@CuO-MWCNTs was used as support of Ab_2 and catalyst for the reduction of hydrogen peroxide. The electrocatalytic reduction of hydrogen peroxide was monitored by amperometry giving a linear range from 1 pg mL^{-1} to 20 ng mL^{-1} and a detection limit of 0.33 pg mL^{-1}. Yang et al. [75] proposed the immobilization of Ab_1 at AuNPs-(3-mercaptopropyl) trimethoxysilane (AuNPs-MPTS) and the use of Ab_2 labeled with HRP and thionine (Ab_2-thionine-HRP) bond to AuNPs-functionalized MWCNTs nanocomposite. AuNPs-MPTS increased the surface area and improved the capture of a larger amount of Ab_1. The catalytic peak current of thionine in the presence of H_2O_2 was used as analytical signal. The proposed sensing strategy provided a stable, selective, and reproducible response with a detection limit of 3 pg mL^{-1}. Feng et al. [76] developed a sandwich-type electrochemical immunosensor for simultaneous detection of CEA and AFP based on the use of modified AuNPs as platform for immobilizing the primary antibodies corresponding to each biomarker and AuNPs-decorated MWCNTs (AuNPs@MWCNTs) as carriers to immobilize a large amount of the both Ab_2 and the two metallic tags, Pb(II) and Cd(II). The multiplexed immunoassay exhibited good sensitivity and selectivity with excellent linear ranges and detection limits for both analytes (detection limits of 3.0 pg mL^{-1} for CEA and 4.5 pg mL^{-1} for

AFP), representing an interesting work for addressing the current requirements of multianalytes detection. The method was successfully used for the quantification of AFP and CEA in human serum samples.

ECL biosensors have also been used for AFP detection. Niu et al. [77] reported an AFP immunosensor based on peroxydisulfate without conventional luminescent reagents by coupling two enzymes to *in situ* generate the co-reactant with PdNPs as catalyst for the ECL reaction peroxydisulfate/O_2. PdNPs were attached to oxidized carbon nanotubes to bind Ab_2 and two enzymes, HRP and GOx. In the presence of glucose, GOx generates H_2O_2 which was subsequently reduced by HRP to *in situ* produce O_2. The assay allowed the detection of AFP at fg mL^{-1} level. Dai et al. [78] reported a biosensing platform based on electrospun carbon nanotubes nanofibers (CNTs@PNFs) composite, which enabled strong ECL emission of peroxydisulfate with favorable analytical performances, (linear range from 0.1 pg mL^{-1} to 160 ng mL^{-1} and detection limit at sub-pg mL^{-1} level.

2.4. Cytokines

Cytokines are small proteins with important roles as cell signaling and immunomodulating agents and their quantification is very important for early prognosis and diagnosis of numerous diseases [79]. In this section, we present different schemes for electrochemical biosensing of several cytokines based on the use of CNTs either in the primary biorecognition platform or as part of the label conjugate.

Tumor necrosis factor-alpha (TNF-α) is a cytokine related to diabetes, graf rejection, and many infectious and inflammatory diseases such as rheumatoid arthritis, HIV infection, neonatal listeriosis, systemic erythema nodosum leprosum, endotoxic shock, and severe meningococcemia [80]. In the last years, some CNTs-based immunosensors have been developed to detect TNF-α. Mazloum-Ardakani et al. reported two label-free immunosensors based on the use of SPE, in one case modified with MWCNTs funtionalized with fullerene (C_{60}) and the ioinic liquid 1-butyl-3-methylimidazolium-bis(trifluoromethylsulfonyl)imide ([C4mimi][NTf2]) (MWCNTs-C_{60}-[C4mimi][NTf2]) [81], and in the other, modified with MWCNTs associated with bimetallic Ag@Pt core-shell NPs and Chit (MWCNTs-Ag@Pt-Chit) [82]. The analytical signals were obtained from the decrease in the oxidation current of catechol due to the surface blockage produced by TNF-α. Linear ranges from 5 to 75 pg mL^{-1} and 6 to 60 pg mL^{-1}, and detection limits of 2 and 1.6 pg mL^{-1}, were obtained for SPE/MWCNTs-C_{60}-[C4mimi][NTf2]/anti-TNF-α and SPE/MWCNTs-Ag@Pt-Chit-anti-TNF-α, respectively. Mazloum-Ardakani et al. [83] also reported a sandwich-type immunosensor prepared by modification of GCE with a nanocomposite based on MWCNTs, AuNPs, and Chit (MWCNTs-AuNPs-Chit) as platform for the immobilization of the anti-TNF-α primary antibody (Ab_1) *via* EDC/NHS chemistry. The detection of TNF-α was performed using an anti-TNF-α secondary antibody (Ab_2) labeled with HRP, H_2O_2 as substrate, and acetaminophen as redox mediator. Compared to the previous platform, the linear range was wider (from 6 to 100 pg mL^{-1}) and the long-term stability was better (96% of the initial response was retained after 30 days). Moreover, the developed immunosensor was successfully used for the determination of TNF-α in spiked serum samples with quantitative recoveries.

Adiponectin (APN), a protein of 244-aminoacids, is an anti-inflammatory cytokine involved in glucose and lipid metabolisms. It is a possible biomarker for the metabolic syndrome and the determination of APN levels is useful for the prevention and treatment of obesity, insulin resistance, hyperlipidemia, and atherosclerosis [84]. Ojeda et al. [85] developed an electrochemical immunosensor for APN based on the use of SPE modified with 4-carboxyphenyl radical grafted-double-walled carbon nanotubes (DWCNTs-Phe-COOH) and the metallic-complex chelating polymer Mix&Go^{TM} for the oriented and stable immobilization of anti-APN primary antibody through the bond of the polymer to Fc-domain antibody as anchoring point. The subsequent sandwich interaction of APN with HRP-labeled anti-APN secondary antibody allowed the detection of APN between 0.05 and 10 μg mL^{-1} with a detection limit of 14.5 ng mL^{-1}. The proposed immunosensor showed high selectivity by testing proteins such as BSA, ceruloplasmin, C-reactive protein (CRP), TNF-α, and ghrelin, and it was successfully used for the determination of APN in human serum.

Interleukins (IL) belong to another important group of cytokines considered as biomarkers for several diseases. Wang et al. [86] developed an immunosensor for the detection of IL-6, a suitable biomarker overexpressed in several types of cancer, including head and neck squamous cell carcinoma. They proposed the use of ITO chips modified with AuNPs-Gr-silica sol-gel as platform for the immobilization of the biorecognition interface. The sandwich-type immunosensor was obtained by using an anti-IL-6 secondary antibody (Ab_2) labeled with HRP and a nanocomposite based on CNTs, AuNPs, and pDA. The detection of IL-6 was performed by amperometry using H_2O_2 as substrate and hydroquinone as redox mediator providing a dynamic working range between 1 and 40 pg mL^{-1} and a detection limit of 0.3 pg mL^{-1}. Yang et al. [87] developed a simple, extremely sensitive, and label-free impedimetric immunosensor for the detection of IL-6. In this case, anti-IL-6 primary antibody (Ab_1) was covalently immobilized at SiO_2/Si modified with horizontally aligned SWCNTs decorated with AuNPs. The immunosensor was highly sensitive making possible the detection of 0.01 fg mL^{-1} IL-6. The immunosensor also demonstrated very good long-term stability since the response remained almost constant even after 1-month storage. This label-free approach gave a considerably better detection level with a relatively simple strategy. Sardesai et al. [88] described the incorporation of a CNTs-based microwell ECL immunoarray into a microfluidic system for the simultaneous detection of PSA and IL-6 in serum samples. SWCNTs forests were assembled at the bottom of the microwells and Ab_1 was attached to their carboxylated ends. The quantification was performed by using Ab_2 modified with $[Ru(bpy)_3]^{2+}$-SiO_2NPs. Ultralow detection limits (100 fg mL^{-1} for PSA and 10 fg mL^{-1} for IL-6) were reached in calf-serum samples. Moreover, PSA and IL-6 were detected in cancer patient serum samples in 1.1 h with very good correlation with ELISA. More recently, Kadimisetty et al. [89] reported a similar protocol to develop an inexpensive automated multiplexed protein immunoarray featuring an on-board microprocessor to control micropumps, and a microfluidic sample/reagent cassette upstream of a microwell ECL immunoarray. They simultaneously detected IL-6, PSA, prostate specific membrane antigen (PSMA), and platelet factor-4 (PF-4) in calf-serum samples with high specificity and selectivity in 36 min, reaching a detection limit of 100 fg mL^{-1}. Sánchez-Tirado et al. [90] recently reported a dual electrochemical immunosensor for the simultaneous determination of IL-1β and TNF-α based on a SPE modified with DWCNTs functionalized with *p*-aminobenzoic acid, which exhibited the oriented immobilization of Ab_1 with the commercial polymeric coating Mix&Go^{TM} and Ab_2 conjugated with poly-HRP (Fig. 4). This immunosensing device made possible the sensitive quantification of both cytokines (detection limits of 0.38 pg mL^{-1} for IL-1β and 0.85 pg mL^{-1} for TNF-α), being adequate for their selective determination in human serum and saliva samples in a very competitive way taking times shorter than the commercial ELISA kit (2.5 h).

Procalcitonin (PCT) is a protein of 116 amino acids with molecular weight of 13 kDa related to inflammatory cytokines. This protein has received great attention as ideal diagnostic indicator

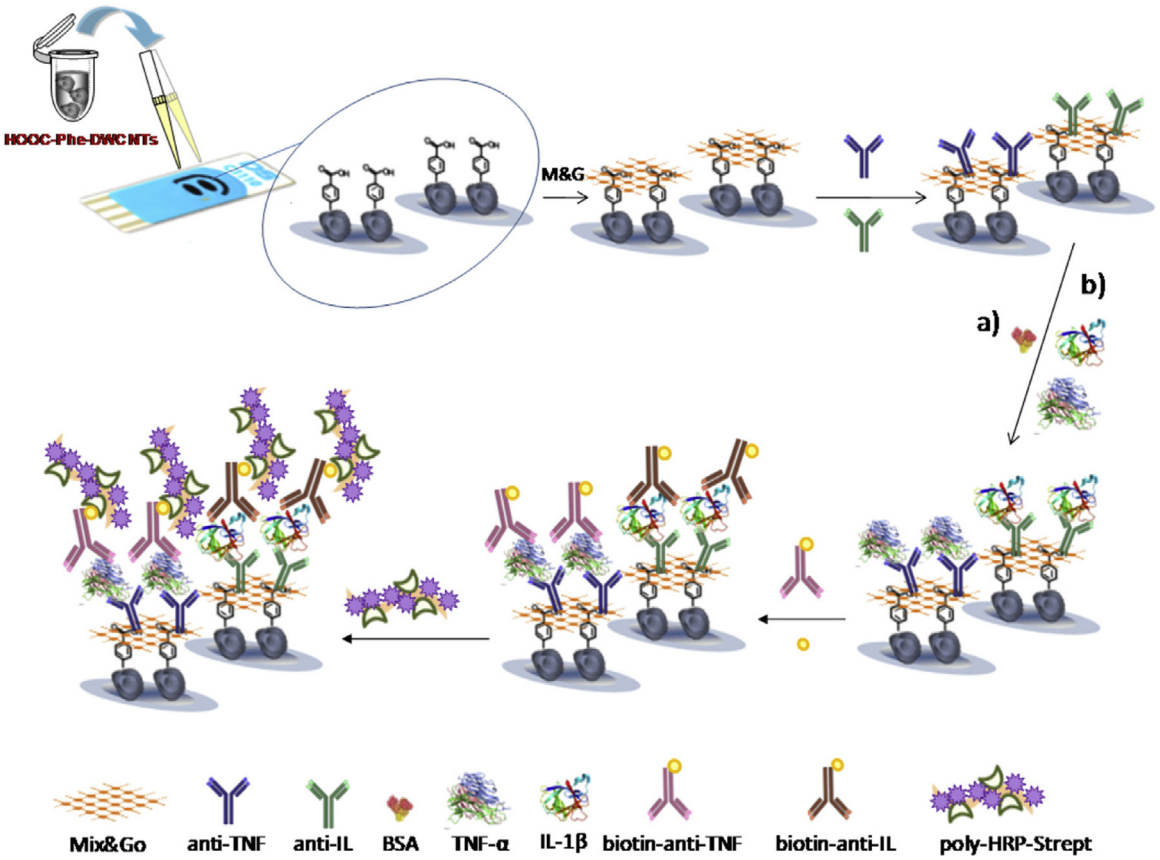

Fig. 4. Schematic display of the different steps involved in the preparation of the dual electrochemical immunosensor for multiplexed determination of IL-1β and TNF-α cytokines.
Reprinted from Ref. [90], Copyright (2017), with permission from Elsevier.

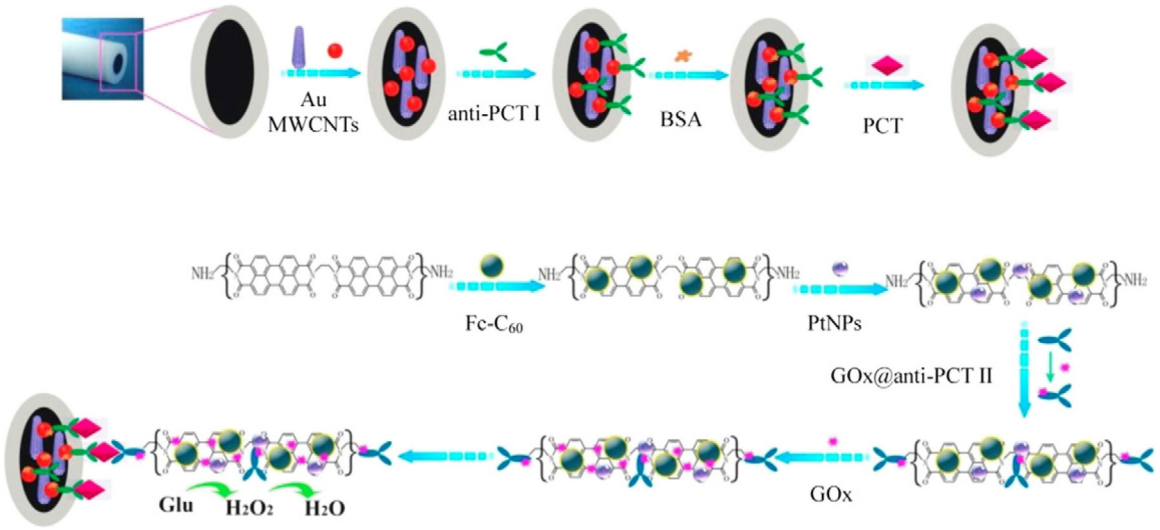

Fig. 5. Schematic diagram for fabrication of an electrochemical immunosensor for the detection of PCT and the corresponding catalysis amplifying principle.
Reprinted from Ref. [92], Copyright (2015), with permission from Elsevier.

of systemic inflammation produced by bacterial infection in early stages [91]. In this context, different CNTs-based electrochemical configurations have been developed for PCT detection. Li et al. [92] used a GCE modified with a MWCNTs-AuNPs nanohybrid as platform to increase the capture of anti-PCT primary antibodies (Ab_1). An interesting amplification scheme was based on the use of an anti-PCT secondary antibody (Ab_2) labeled with GOx and a nanocomposite containing fullerene C_{60}, Fc, and PtNPs (C_{60}-Fc-PtNPs-GOx). The hydrogen peroxide generated after the addition of glucose was further reduced by C_{60}-Fc-PtNPs nanocomposite (Fig. 5). This amplification scheme allowed detecting PCT in the range of 0.01–10 ng mL^{-1}, with a detection limit of 6 pg mL^{-1}. Yang et al. [93] reported a similar scheme using a nanohybrid based on MWCNTs functionalized with cobalt phthalocyanine nanoparticles

(MWCNTs-CoPcNPs) and choline oxidase (ChOx) as label of Ab_2. ChOx catalyzes the oxidation of choline with production of H_2O_2, which is then oxidized at MWCNTs-CoPcNPs, without the addition of other redox mediators, resulting in an important amplification. The proposed immunosensor exhibited a wide linear range (from 0.01 to 100 ng mL^{-1}) and a detection limit of 1.23 pg mL^{-1}, with no cross-reactivity with carbohydrate antigen 19-9 (CA19-9), BSA, and human cytomegalovirus (HCMV). Liu et al. [94] prepared a sandwich-type immunosensor based on a GCE modified with ERGO and AuNPs for Ab_1 immobilization, and Ab_2 labeled with a complex of single-walled carbon nanohorns and hollow Pt chains. The use of thionine and HRP allowed the amplification of the catalytic activity giving a linear range from 0.001 to 20 ng mL^{-1}, and a detection limit of 0.43 pg mL^{-1}. Fang et al. [95] developed a platform based on the layer-by-layer modification of GCE with Gr, MWCNTs, and Chit for the immobilization of Ab_1 *via* glutaraldehyde reaction. The amplification was obtained using an Ab_2 labeled with a conjugate based on mesoporous silica MCM-41 modified with thionine, AuNPs, and HRP. The authors reported a wide linear range, from 0.01 to 350 ng mL^{-1}, with a detection limit of 0.5 pg mL^{-1} and successful application in serum samples.

2.5. Cardiac biomarkers

Cardiovascular disease (CVD) includes several heart and circulation pathologies like coronary heart disease, angina, heart attack, congenital heart disease, and stroke. CVD represents 46.2% of death due to non-communicable diseases according World Health Organization (WHO) statistics [96]. Therefore, early and quick diagnosis is crucial for successful prognosis of these diseases. One of the criteria of WHO for the diagnosis of CVD is the elevation of the biochemical markers in blood samples.

Cardiac markers are proteins that leak out of injured myocardial cells through their damaged membranes into the blood stream [97,98]. Elevated concentrations of these cardiac markers in serum are associated with recurrent CVD events and higher death rates. At present, there are four biomarkers established for the diagnosis of myocardial infarction (MI)-related CVD: cardiac troponin I (cTnI) and T (cTnT), MB isoform of creatine kinase (CK-MB), and myoglobin (Mb) [99]. Mb is the cardiac biomarker that changes more rapidly after cardiac injury. Due to its small size (17.8 kDa), it is quickly released into circulation (as early as 1–3 h upon onset of symptoms) reaching the maximum 6–12 h after [100]. The expression level of Mb increases up to ~600 ng mL^{-1} (the normal range goes from 50 to 200 ng mL^{-1}). The muscle isoenzyme CK-MB is specific for cardiac injury and its level in serum becomes abnormal within 4–6 h after onset of acute MI, peaking at 18–24 h in the range of 39–185 ng mL^{-1} [101,102]. cTnT and cTnI are more sensitive and specific than Mb and CK-MB [103]. Both are released from the death cell within 2–4 h and 3–4 h, respectively, after the onset of MI symptoms. In principle, cTnT and cTnI remain in the blood stream more than 10 days, reaching the maximum concentration approximately 1–2 days after myocardial injury, becoming useful diagnosing tools for sub-acute MI. In normal patients, the level of cTnI is around 0.001 μg L^{-1} increasing to 100 μg L^{-1} in MI patients [104]. Even a concentration as low as 0.01 μg L^{-1} can be related to heart failure.

Table 4 displays the analytical parameters of the cardiac biomarkers-immunosensors based on CNTs published in the period covered by this review. Most of the lately reported CNT-based electrochemical biosensors for cardiac biomarkers relied on the use of antibodies as biorecognition elements [105–109]. In these cases, the target biomarker binds specifically to a primary biomarker antibody attached to CNTs at the electrode surface. As in previous cases, the detection is performed indirectly either using an outer redox probe or an enzyme-linked secondary antibody. Due to the electrocalytic properties of CNTs toward the usual redox probes $[Fe(CN)_6]^{3-/4-}$ and H_2O_2, the detection limits reported for cTnT [105,106], cTnI [107–109], CK-MB [109], and Mb [109] are perfectly suited for their detection in the relevant clinical concentration intervals.

Some other non-immunosensing strategies based on the use of aptamers and MIP as (bio)recognition elements and CNTs have been reported. A summary of the analytical parameters of these cardiac biomarkers aptasensors and MIP-sensors is presented in Table 4. Kumar et al. [110] developed a label-free aptamer-based electrochemical biosensor by drop-casting an anti-Mb aptamer at a SPE modified with an hybrid of rGO and MWCNTs. The selective affinity interaction between the aptamer and Mb allowed the efficient immobilization of the protein at the electrode. The quantification was performed from the direct reduction of Fe(III)-hem to Fe(II)-hem at around −0.5 V (Fig. 6). The assay showed a dynamic response range between 1.0 ng mL^{-1} and 1 μg mL^{-1} and a detection limit of 0.34 ng mL^{-1}. Ma et al. [111] developed a MIP at a MWCNTs-based GCE electrode for selective determination of cTnI. This electroactive platform was fabricated by depositing Gr nanoplatelets, MWCNTs, and Chit followed by the interaction with the template cTnI protein using glutaraldehyde overnight. Afterwards, MIP polymer was synthesized using methacrylic acid as the monomer, ethylene glycol dimethacrylate as the cross-linker, and α-α′-azobisisobutyronitrile as the initiator. The detection of the cardiac biomarker was made by comparing the DPV peak of $[Fe(CN)_6]^{3-/4-}$ before and after the recognition of the target protein. This methodology presented a detection limit of 0.8 pg mL^{-1} and the platform retained its response after 14 days of continuous use by washing the adsorbed cTnI with a methanol:acetic acid solution (9:1 v/v). As it was previously mentioned, the use of aptasensors represent an interesting and very promising alternative to immunosensors for the quantification of cardiac biomarkers.

2.6. Other protein biomarkers

Insulin growth factor-1 (IGF-1), a peptide hormone of 70 amino acid residues plays important roles in several human malignancies contributing to unregulated cell proliferation. Serafin et al. [112] reported for the first time an electrochemical immunosensor for the determination of IGF-1. GCE modified with MWCNTs and electrogenerated poly(pyrrole propionic acid) was used as transducer providing a high content of carboxyl groups for the immobilization of the anti-IGF-1 primary antibody (Ab_1) *via* carbodiimide coupling method. The transduction of the biorecognition event was performed by amperometry using an anti-IGF-1 secondary antibody (Ab_2) labeled with HRP, catechol as redox mediator and H_2O_2 as substrate. The proposed immunosensor showed a wide linear range from 0.5 to 1000 pg mL^{-1}, and a detection limit more than one hundred times lower than the one reported for ELISA kits (0.25 pg mL^{-1}). This new immunosensor was successfully used for the determination of IGF-1 in spiked serum samples with excellent recoveries.

β-Galactoside-α-2,6-sialyltransferase (ST6Gal-I) is another important cancer biomarker. It is member of sialyltransferases family and it is a critical regulator of tumor cell survival by inhibiting a multiplicity of cell death pathways [113]. Zhang et al. [114] developed a novel electrochemical immunosensor for ST6Gal-I detection based on the modification of GCE with a PB-hybrid material containing GO, PB nanoparticles (PBNPs), PTA (an aminated derivative of 3,4,9,10-perylenetetracarboxylicdianhydride), MWCNTs, and Chit. The high density of amine groups at chitosan and PTA allowed the adsorption of AuNPs onto the surface of the nanocomposite, providing a large surface area that facilitated the immobilization of anti-ST6Gal-I primary antibody. The affinity recognition of ST6Gal-I was monitored from the PB DPV signal with

Table 4
CNTs-based electrochemical biosensors for cardiac biomarkers.

Biomarker	Platform	Technique/Methodology of detection	Linear range detection limit	Comments	Ref.
cTnT	SPE-MWCNTs-NH_2/Ab	DPV: indirect determination *via* change in $[Fe(CN)_6]^{3-/4-}$ current	0.0025–0.5000 ng mL^{-1} 0.0035 ng mL^{-1}	Calibration plot was also made in serum samples and confronted with ECLIA	[105]
cTnT	AuE/PEI/cMWCNTs/Ab	CV: indirect determination with anti-cTnT-HRP coupled to the platform, using H_2O_2 as mediator	0.1–10.0 ng mL^{-1} 0.033 ng mL^{-1}	Calibration plot was also made in serum samples and confronted with ECLIA	[106]
cTnI	GCE/Gr-MWCNTs/PyBu/Ab	EIS: indirect determination *via* change in $[Fe(CN)_6]^{3-/4-}$ R_{ct}	0.001–10.0 ng mL^{-1} 0.94 pg mL^{-1}	Sampled interferents: serum sample spiked with IgG and CRP Real sample: serum sample spiked with cTnI	[107]
cTnI	GCE/Gr-MWCNTs/PyMA/MPA-PtNPs/Ab	EIS: indirect determination *via* change in $[Fe(CN)_6]^{3-/4-}$ R_{ct}	0.001–10.0 ng mL^{-1} 1.0 pg mL^{-1}	Sampled interferents: IgG and CRP Real sample: serum sample spiked with cTnI	[108]
Mb	GCE/MWCNTs-SU8/Ab	EIS: indirect determination *via* change in $[Fe(CN)_6]^{3-/4-}$ R_{ct}	1.0–50.0 ng mL^{-1} 0.1 ng mL^{-1}	—	[109]
cTnI	GCE/MWCNTs-SU8/Ab		0.1–10.0 ng mL^{-1}		
CK-MB	GCE/MWCNTs-SU8/Ab		10.0 ng mL^{-1}–10.0 μg mL^{-1}		
Mb	SPE/rGO-MWCNTs/Aptamer	CV: direct determination through electron transfer of Mb heme group.	1–1024 ng mL^{-1} 0.34 ng mL^{-1}	Sampled interferents: BSA and Hb	[110]
cTnI	GCE/Gr-MWCNTs-Chit/MIP	DPV: indirect determination *via* change in $[Fe(CN)_6]^{3-/4-}$ current	0.005–10.0 ng mL^{-1} 0.8 pg mL^{-1}	Sampled interferents: CEA, NSE, BSA, p24, and HCG. Real sample: serum sample spiked with cTnI	[111]

Abbreviations: cTnT: cardiac troponin T; SPE: screen printed electrode; MWCNTs-NH_2: aminated multi-walled carbon nanotubes; Ab: capture antibody; DPV: differential pulse voltammetry; ECLIA: electrochemical chemiluminescence immunoassay; AuE: gold electrode; PEI: polyethyleneimine; cMWCNTs: carboxylated multi-walled carbon nanotubes; CV: cyclic voltammetry; HRP: horseradish peroxidase; cTnI: cardiac troponin I; GCE: glassy carbon electrode; Gr: graphene; PyBu: 1-pyrenebutyric acid; EIS: electrochemical impedance spectroscopy; IgG: immunoglobulin-G; CRP: C-reactive protein; PyMA: 1-pyrenemethylamine; MPA: mercaptopropionic acid; PtNPs: platinum nanoparticles; Mb: myoglobin; SU8: epoxy-based negative photoresist; CK-MB: MB isoform of creatine kinase; rGO: reduced graphene oxide; BSA: bovine serum albumin; Hb: hemoglobin; Chit: chitosan; MIP: molecularly imprinted polymer; CEA: carcinoembryonic antigen; NSE: neuron specific enolase; p24: human immunodeficiency virus p24; HCG: human chorionic gonadotropin.

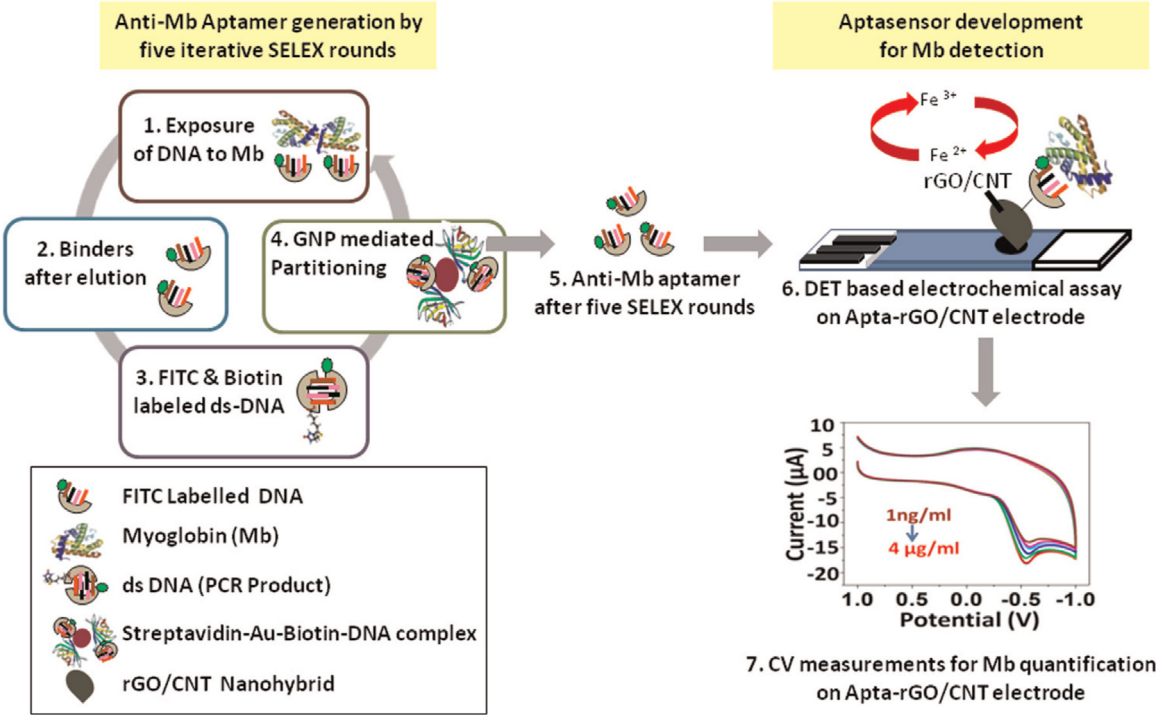

Fig. 6. Scheme showing the streptavidin labeled gold nanoprobes mediated SELEX method for specific anti-Mb aptamer generation (left) and its subsequent usage in the development of rGO/CNT modified aptasensor for the label free detection of Mb (right).
Reprinted from Ref. [110], Copyright (2015), with permission from Elsevier.

a detection limit as low as 3 pg mL^{-1}, attributed to the electrocatalytic effect of the PB-based hybrid nanocomposite and AuNPs.

3. Carbon nanotubes-based electrochemical (bio)sensors for nucleic acids biomarkers

3.1. microRNA

microRNAs (miRNAs) were discovered more than 20 years ago [115]. The term microRNA or miRNA was introduced in 2001 in order to describe these short (19–25 nucleotides) non-coding ribonucleic acid (RNA) molecules that regulate gene expression by repression of messenger RNA (mRNA) translation or by mRNA degradation at the post-transcriptional level [116]. More than 60% of human protein-coding genes are under miRNA regulation; that is the reason for the outstanding importance of miRNAs in gene regulation [117]. A single miRNA molecule can regulate hundreds of mRNAs and, therefore, it has power over a whole expression network [118,119]. Consequently, due to this enormous regulatory power, abnormal miRNAs expression levels have been involved in several pathologies including neurodegenerative diseases and central nervous system injury [120,121], diabetes [122,123], cardiovascular [124,125], kidney [126–128], and liver [129–133] diseases, and even immune dysfunction [134–136]. In this sense, several miRNAs have been already reported as reliable markers for diagnosis and prognosis since they are present in different body fluids (blood, saliva, urine) in stable form allowing non-invasive extraction ways [120,122,126,132]. Thus, the quantification of the expression levels of one, or more commonly, a set of miRNAs, has significant clinical relevance and strong impact on health care [137]. Table 5 summarizes the analytical characteristics of the most representative CNTs-based miRNA electrochemical biosensors reported between 2013 and 2017.

In 2013, Ramnani et al. [138] developed an original and specific electronic detection of miRNA at attomolar level using a SWCNTs field-effect transistor involving the specific interaction between the protein p19 and double stranded RNA (dsRNA) sequences. The authors used as a model miRNA-122a, a specific liver marker expressed in 70% of liver cells [131], which is involved in lipid metabolism and liver homeostasis [139] and hepatitis C virus replication [130]. p19 is a small protein (19 kDa) which binds with high affinity only to dsRNA [140,141]. This molecular recognition is size-specific and sequence-independent and presents the highest affinity for dsRNA sequences of 21–23 bases whereas the affinity decreases for sequences longer than 23 bases and shorter than 19. The design of the nanobiosensor was based on microfabricated interdigitated gold electrodes acting as source and drain on Si/SiO_2 modified by SWCNTs networks attached by using 3-aminopropyltriethoxy silane to bridge the interdigitated electrodes, followed by the platform modification with p19. The decrease in the currents of I-V profiles was used as analytical signal. This label-free nanobiosensor was able to perform the selective and sensitive detection of miRNA-122a between 1 aM and 10 fM miRNA in a million-fold excess of other nucleic acids.

Tran et al. [142] proposed two sensing strategies for miRNA-141 as prostate cancer biomarker. In the first one, the label-free and reagentless sensing approach was based on the use of an interpenetrated network of cMWCNTs and an electroactive polymer with embedded quinone groups in the backbone, and further covalent attachment of the DNA probe. The analytical signal was obtained from the changes in the electrochemical response of quinone groups. The biosensor allowed the selective discrimination of miRNA-141 in the presence of non-complementaries miRNA (*i.e.* miRNA-103, colorectal cancer or miRNA-29b as lung cancer biomarkers) with a detection limit of 8 fM. The biosensor presented the disadvantage of the incapacity for the detection of low concentrations of miRNA-141 (10 fM) added to diluted normal serum samples. The second approach to quantify miRNA-141 involved an electrochemical ELISA-like immunosensor based on a screen-printed gold electrode (SPAuE) modified with rGO and cMWCNTs [143] followed by the covalent immobilization of an NH_2-modified DNA probe. Once the hybridization took place, the detection of miRNA-141 proceeded with the addition of anti-RNA.DNA primary antibody (Ab_1) and further association of HRP-conjugated anti-RNA.DNA secondary antibody (Ab_2-HRP). The electrochemical signal was obtained by SWV in the presence of H_2O_2 and hydroquinone, and the detection limit obtained under these conditions was 30 fM. Li et al. [144] proposed two biosensing approaches based on oxidized-MWCNTs for miRNA-24, which is involved in cell proliferation [145,146] and cancer cell differentiation [146]. The first strategy [144] was based on the use of GCE modified with cMWCNTs as support for the covalent attachment of DNA probe and allowed the detection of pM levels of the miRNA. The analytical signal was obtained by DPV from the oxidation of guanine residues at GCE/cMWCNTs. The biosensor was challenged with total RNA extracted from human cultured cervical cancer (HeLa) cells samples enriched with miRNA-24, showing good recovery (108.9%) although the reproducibility was limited (RSD of 15.6%). The other approach presented by these authors was focused on the use of a PAMAM dendrimer covalently attached to cMWCNTs dropped onto GCE as platform for the covalent immobilization of the 5′-carboxyl modified capture-DNA probe using MB as redox indicator [147]. The presence of PAMAM modified-MWCNTs hybrids contributed to the increase of the amount of capture-DNA probe and, therefore, to the enhancement of the MB mediated detection signal. In addition, PAMAM functionalization minimized the unspecific adsorption of MB on cMWCNTs surface. The estimated detection limit was 0.5 fM although the biosensor demonstrated limited selectivity. Recovery assays for miRNA-24 in total RNA sample (HeLa cells) presented very good correlation with quantitative PCR detection results. Liu et al. [148] developed an ultrasensitive electrochemical biosensor for miRNA-21, a biomarker implicated in cell cycle regulation and apoptosis and associated with several types of cancer [149–151]. The biosensor was prepared using a 3D layer-by-layer nanostructure containing oxidized-SWCNTs and nanodiamonds on gold electrodes and AuNPs deposited on the last layer of oxidized-SWCNTs. The resulting platform was modified by tetrahedral DNA nanostructures that have mechanical rigidity and structural stability and allows the effective anchoring of a diversity of targets. The amplification strategy was obtained by addition of DNA-functionalized AuNPs modified with long hemin-G-quadruplex DNAzyme nanowires, which exhibit peroxidase activity (Fig. 7). This biosensing system displayed a linear relationship between reduction current and $\log C_{\text{miRNA-21}}$ from 10 fM to 1 nM and a detection limit of 1.95 fM. The biosensor presented excellent stability for 2 weeks at 4 °C. Although recovery assays using serum samples enriched with miRNA-21 gave excellent results, the biosensor failed on the detection of mismatches sequences. Rafiee-Pour et al. [152] presented another electrochemical biosensor for miRNA-21, using GCE modified with a dispersion of cMWCNTs in DMF as support for the covalent attachment of ssDNA probe and MB as redox marker. The analytical signal was obtained by DPV from the changes in MB oxidation currents after the hybrid formation. A linear relationship was obtained in the range of 0.1–500 pM with a detection limit of 84.3 fM, with good discrimination of a mismatch target.

3.2. DNA

Circulating cell-free DNA holds promise as a new generation of biomarkers for a variety of clinical, environmental, and food

Table 5
CNT-based electrochemical biosensors for microRNAs.

miRNA biomarker	Platform	Detection	Linear range detection limit	Sample	Comments	Ref.
dsRNA(miRNA-122a/probe)	Silicon/SiO_2/Ti/ Au/SWCNTs/p19	FET	1 aM to 10 fM 1 aM	Total RNA from yeast	- Very high specificity: detection of miRNA-122a in a million fold-excess of other nucleic acids	[138]
miRNA-141	GCE/cMWCNTs/poly (JUG-co-JUGA)/ODN probe	SWV	1 fM to 100 pM 8 fM	2% diluted serum solution	- Unspecific physisorption of serum proteins on platform	[142]
miRNA-141	SPAuE/rGO/cMWCNTs/ODN-141-P/miRNA-141/Ab_1/Ab_2-HRP	SWV	10 fM to 10 nM 30 fM	—	- Good specificity: recognition of miRNA-141 from non-complementary miRNA-29b target	[143]
miRNA-24	GCE/cMWCNT/NH_2-DNA probe	DPV	1 pM to 1 nM 1 pM	Total RNA from HeLa cells	- Good specificity: recognition of miRNA-24 from non-complementary miRNA-29 target, no discrimination of central single base-mismatched miRNA-24	[144]
miRNA-24	GCE/cMWCNT-PAMAM/probe + MB	DPV	10 fM to 1 nM 0.5 fM	Total RNA from HeLa cells	- Good specificity: recognition of miRNA-24 from non-complementary miRNA-29 target, somewhat discrimination of central single base-mismatched miRNA-24 - Detection of miRNA-24 comparable with quantitative PCR	[147]
miRNA-21	Au/oxSWCNTs/ND/ oxSWCNTs/depAuNPs/TSPs	DPV	10 fM to 1 nM 1.95 fM	Serum	- High specificity: recognition of miRNA-21 from single-base, two-base and three-base mismatch oligonucleotides, non-complementary target, miRNA-126, and miRNA-141 - Good stability: 2 weeks stored at 4 °C - Recovery assays from 99.3% to 101.6%	[148]
miRNA-21	GCE/cMWCNT/ss-DNA + MB	DPV	0.1 to 500 pM 84.3 fM	—	- Good specificity: recognition of miRNA-21 from non-complementary miRNA-192 target	[152]

Abbreviations: SWCNTs: single walled carbon nanotubes; p19: RNA binding protein from Carnation Italian ringspot virus; FET: field-effect transistor; GCE: glassy carbon electrode; cMWCNTs: carboxylated multi-walled carbon nanotubes; JUG: 5-hydroxy-1,4-naphthoquinone monomer; JUGA: 3-(5-hydroxy-1,4-dioxo-1,4-dihydronaphthalen-2(3)-yl) propanoic acid monomer; poly (JUG-co-JUGA): JUG and JUGA polymer; ODN probe: amino-modified DNA probe; SWV: square-wave voltammetry; SPAuE: gold screen-printed electrodes; rGO: reduced graphene oxide; ODN-141-P: amino-modified DNA; Ab_1: anti-RNA.DNA primary antibody; Ab_2: anti-RNA.DNA secondary antibody; HRP: horseradish peroxidase; PAMAM: polyamidoamine dendrimer; probe: 5′-carboxyl-modified capture DNA probe; MB: methylene blue; Au: Gold electrode; oxSWCNTs: oxidized single walled carbon nanotubes; ND: nanodiamonds; depAuNPs: deposited gold nanoparticles; TSPs: DNA tetrahedron-structured nanowire probe with DNAzyme activity; ss-DNA: DNA probe.

applications including the diagnostic and prognostic of cancer and the detection of bacteria, parasites, and viruses. For this reason, the interest in the detection and quantification of specific DNA sequences has grown tremendously in the last decade. In the following section, we present the most relevant CNTs-based genosensors for DNA biomarkers reported between 2013 and 2017. The most significant information about their analytical characteristics is summarized in Table 6.

Wang et al. [153] developed a novel electrochemical impedimetric genosensor for the quantification of PML-RAR alpha fusion gene, which represents a specific tumor marker for the diagnosis and monitoring of acute promyelocytic leukemia. This genosensor was obtained *via* (i) the modification of GCE with a DWCNTs-ethylenediamine-FePtNPs suspension (GCE/DWCNTs-en-FePtNPs) to enhance the conductivity and surface area, and (ii) the immobilization of a 18-base single strand DNA sequence (DNA probe) at the resulting GCE/DWCNT-en-FePtNPs. The hybridization was determined from EIS through the changes in R_{ct} of $[Fe(CN)_6]^{3-/4-}$. This genosensor was highly sensitive and reproducible, and reached a detection limit of 0.1 pM.

Fayazfar et al. [154] also used EIS for the detection of a 26-base fragment of the TP53 tumor suppressor gene, the most frequently mutated gene in human cancer, which is exploited in the clinics as biomarker for early detection, diagnosis, and prognosis of breast, colon, and lung cancer. The authors proposed a bioplatform based on the electrochemical growth of AuNPs on the vertically aligned MWCNTs array deposited onto tantalum electrodes (TaE). This strategy provided synergistic interactions of aligned MWCNTs and AuNPs, which improve the density of the DNA probe attachment and the analytical performance of the resulting DNA biosensor. In fact, this impedimetric genosensing device presented: (a) high selectivity (able to distinguish one-base mismatched); (b) very high sensitivity (detection at attomolar level (10 aM)), and (c) wide linear range (1.0×10^{-15} to 1.0×10^{-7} M). These analytical characteristics make the device highly competitive, with clear analytical superiority over other electrochemical biosensors reported for the detection of TP53 gene mutation.

Wang et al. [155] designed hybridization-based impedimetric sensors for recognition of DNA sequences related to both hepatitis B virus (HBV) and human papillomavirus (HPV). These label-free genosensing platforms were developed by electrochemical deposition of AuNPs on SWCNTs arrays prepared *in situ* onto SiO_2/Si wafer, followed by self-assembly of the corresponding thiolated ssDNA probe onto the SWCNTs/AuNPs platform. A linear

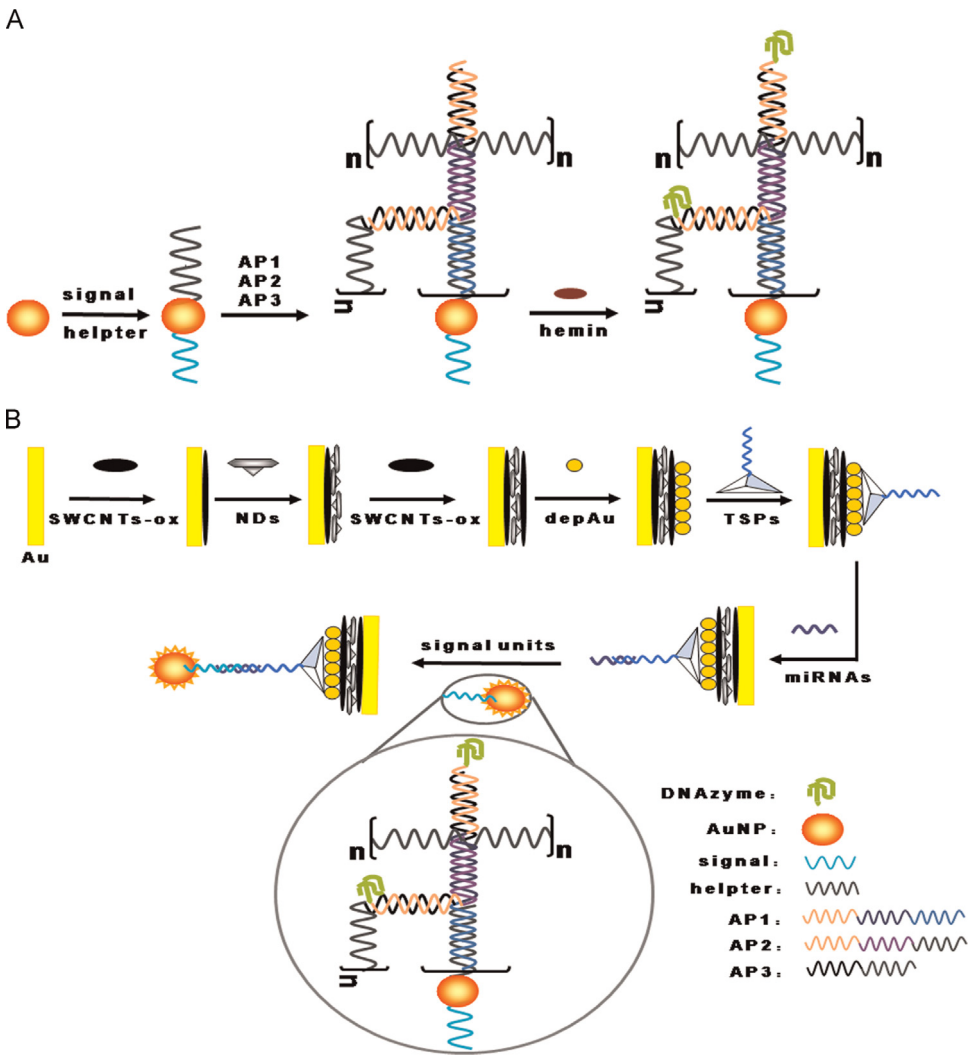

Fig. 7. Schematic illustrations of the electrochemical biosensor fabrication process for detection of miRNA-21. *Note*: *n* represents the number of cycles. Reprinted from Ref. [148], Copyright (2015), with permission from Elsevier.

relationship between the change in R_{ct} of $[Fe(CN)_6]^{3-/4-}$ and the logarithm of HBV-ssDNA concentration was obtained in the range from 1 aM to 1 μM, with a detection limit of 1 aM. For HPV biosensing, the linear relationship ranged between 1 aM and 1 pM, and the detection limit was the same as the one obtained for HBV DNA.

Lee et al. [156] reported a new electrochemical DNA assay for the determination of the P185 BCR-ABL oncogene. This oncogene is a valuable molecular marker because it is found in most Philadelphia chromosome-positive patients with acute lymphocytic leukemia and serves as a specific genetic biomarker for the early relapse detection, prognosis, and therapeutic decision-making [157]. Fig. 8 displays a schematic representation of the protocol for P185 BCR-ABL oncogene biosensing. Capture DNA probes immobilized on carboxylated magnetic beads allowed the recognition of a specific region (373–390 bp) of the DNA target. After hybrid formation, the secondary DNA sequence tagged with (CNTs-HRP)-based labels hybridized with another region (401–418 bp) of P185 BCR-ABL oncogene (Fig. 8A). After the sandwich hybridization event took place, the analytical signal was obtained at SPE (Fig. 8B) by SWV from the reduction of the enzymatic product of 2-aminophenol (2-AP) generated by HRP in the presence of H_2O_2. The proposed assay showed an excellent sensitivity (Fig. 8C), a detection limit of 1.7 pM, and an efficient discrimination between the target and a three-base mismatch sequence, resulting in a very interesting alternative to the real-time quantitative polymerase chain reaction methods for the quantification of P185 BCR-ABL oncogene.

4. Carbon nanotubes-based electrochemical (bio)sensors for dopaminergic biomarkers

4.1. Dopamine

There are more than 100 recognized neurotransmitters, the most representative being dopamine (Do), serotonine, epinephrine, norepinephrine, acetylcholine, glutamate, nitric oxide and tryptamine [160]. Considering the great importance of Do and the enormous attention received by electroanalytical chemists, in this review we discuss CNTs-based electrochemical (bio)sensors for Do quantification. Do is an important biomarker for different pathologies. In fact, elevated levels of Do have been associated with neurological disorders like Parkinson's, Alzheimer's, and Huntington's diseases, Tourett'e syndrome, schizophrenia, and psychosis [161]. Dopaminergic neurotransmission plays a major role in motivation, learning/cognition, movement regulation, and addictive behavior [161]. Drugs such as nicotine, amphetamine, cocaine, and ecstasy, change the Do levels and, in some cases, damage the monoaminergic system producing drug addiction with severe social and psychological consequences. The basal levels of

Table 6
CNTs-based electrochemical biosensors for DNA.

DNA biomarker	Platform	Technique/Methodology of detection	Linear range detection limit	Comments	Ref.
PML-RAR alpha fusion gene (acute promyelocytic leukemia)	GCE/DWCNTs-en-FePtNPs/DNA probe	EIS: indirect determination *via* ΔR_{ct} of $[Fe(CN)_6]^{3-/4-}$	1.0×10^{-12} to 1.0×10^{-7} M 2.1×10^{-13} M	- Interelectrode reproducibility: RSD = 4.25%, $n = 6$ - Reusability *via* dehybridization in boiling water for 10 min	[153]
TP53 tumor suppressor gene (several type of human cancers)	TaE/aMWCNTs-AuNPs/DNA probe	EIS: indirect determination *via* ΔR_{ct} of $[Fe(CN)_6]^{3-/4-}$	1.0×10^{-15} to 1.0×10^{-7} M 1.0×10^{-17} M	- High specificity - Interelectrode reproducibility: RSD = 2.1%, $n = 5$ - Good stability: 2 weeks stored at 4 °C - Reusability *via* dehybridizationin hot water (80 °C) for 5 min	[154]
Hepatitis B virus DNA Human papillomavirus DNA	SiO_2/Si/SWCNTs-AuNPs/DNA probe	EIS: indirect determination *via* ΔR_{ct} of $[Fe(CN)_6]^{3-/4-}$	1×10^{-18} to 1×10^{-6} M 1×10^{-18} M 1×10^{-18} to 1×10^{-12} M 1×10^{-18} M	- Very good stability: 4 weeks stored at 4–8 °C - Reusability *via* dehybridization in hot water	[155]
P185 BCR-ABL oncogene (acute lymphocytic leukemia)	- Functionalized magnetic bead/capture DNA probe - Label: cSWCNTs-HRP-detection DNA probe - Electrode: SPE	SWV: indirect determination *via* reduction current of 3-APZ[a]	8.0×10^{-12} to 2.0×10^{-10} M 1.7×10^{-12} M	- High specificity - Interelectrode reproducibility: RSD = 7.7%, $n = 8$	[156]
mga gene of *Streptococcus pyogenes* (rheumatic heart disease)	SPE/cMWCNTs/DNA probe	DPV: indirect determination *via* oxidation current of MB	Up to 0.33 ng μL^{-1} 0.0023 ng μL^{-1}	- High specificity - Excellent stability: 24 weeks stored at 4 °C - DNA target isolated from patients with *S. pyogenes* infection	[158]
Hypermethylated glutathione-S-transferase P1 gene (prostate cancer)	SPE/cMWCNTs/DNA probe	DPV: direct determination *via* oxidation current of guanine bases	– 5.4×10^{-8} M	- High specificity - Interelectrode reproducibility: RSD = 10.8%, $n = 3$ - Very good stability: 6 weeks stored at 4 °C - Reusability *via* dehybridization at applied potential of +1.8 V	[159]

Abbreviations: GCE: glassy carbon electrode; DWCNTs: double-walled carbon nanotubes; en: ethylenediamine; FePtNPs: iron-platinum nanoparticles; EIS, electrochemical impedance spectroscopy; ΔR_{ct}, charge transfer resistance change; TaE, tantalum electrodes; aMWCNTs: aligned multi-walled carbon nanotubes; AuNPs: gold nanoparticles; cSWCNTs: carboxylated single-walled carbon nanotubes; HRP: horseradish peroxidase; SPE: screen printed electrode; SWV: square-wave voltammetry; 3-APZ: 3-aminophenoxazone; 2-AP: 2-aminophenol; cMWCNTs: carboxylated multi-walled carbon nanotubes; DPV: differential pulse voltammetry; MB: methylene blue.

[a] Electroactive reaction product of the HRP-catalyzed oxidation of 2-AP by H_2O.

extracellular Do are around 0.01 and 0.03 μM and in the phasic release during a burst of neuronal firing they can reach 0.1–1 μM [162]. Therefore, it is necessary to have selective and fast methodologies that allow the quantification of Do at nanomolar levels. In this sense, CNTs-based electrochemical sensors have allowed the nanomolar detection of Do not only in pure solutions but also in biological samples with *in vivo* non-invasive applications [61]. Table 7 summarizes the most representative strategies reported between 2013 and 2017 for the electrochemical quantification of nanomolar levels of Do using CNTs-based electrochemical (bio)sensors.

One important strategy to build CNTs-based Do electrochemical sensor is the direct growth of CNTs by chemical vapor deposition since the resulting coatings are more homogenous than those obtained using the conventionally used methods such as dip coating and drop-casting [163,164]. For instance, Sansuk et al. [163] used networks of pristine SWCNTs onto insulating Si/SiO_2 substrates for flow injection analysis (FIA) with electrochemical detection of Do in artificial cerebral fluid with a very good detection limit of 0.05 nM.

The oxidation of CNTs have been also used to build successful electrochemical (bio)sensors. For example, the use of MWCNTs oxidized in basic media demonstrated a very good electrocatalytic activity toward the oxidation of Do [165], showing better detection limits than those obtained using CNTs oxidized in acidic media [166] mainly due to the advantages offered by the basic treatment that preserve the integrity of the tubes and produced highly purified nanomaterials [167].

In the last years, (bio)polymers of different nature have been used for the functionalization of CNTs. It has widely demonstrated that polymers can modify the physical and chemical properties of CNTs, provide them of useful functional groups able to interact with Do (such as –COOH, –CN, $–NH_2$, –SH), and facilitate their deposition at electrode surfaces. The strategy used to produce these polymer-CNTs composites is very important to modulate the electrochemical properties toward Do detection and the performance of the resulting sensors [168–176]. Gutiérrez et al. [168] proposed the modification of GCE with SWCNTs covalently functionalized with polylysine. The selection of the polymer and the strategy

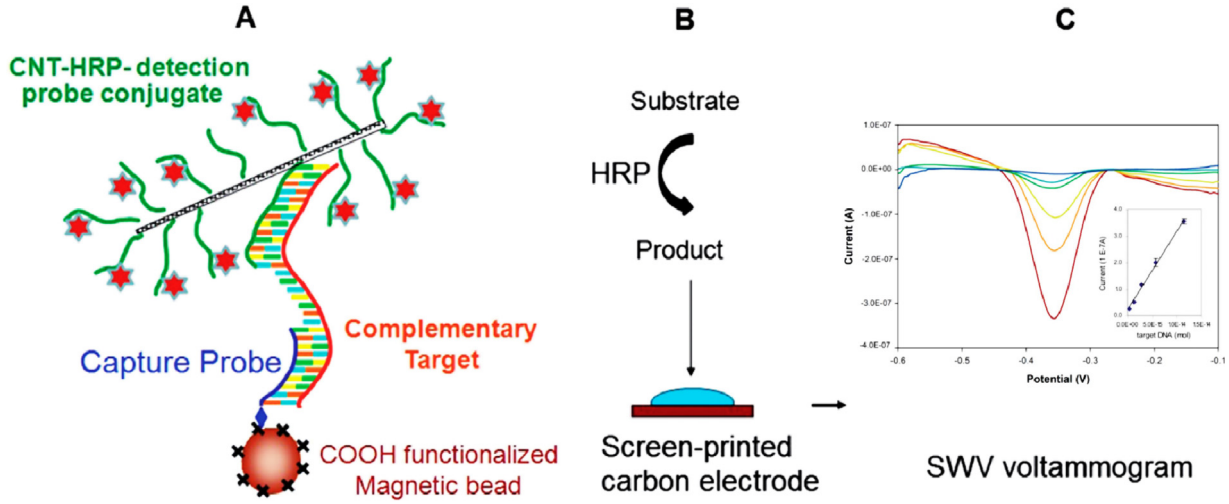

Fig. 8. Schematic representation of signal-amplified electrochemical detection of DNA target using cSWCNT-based labels: (A) Sandwich hybridization assay performed on magnetic beads. (B) The targets were quantified by measuring the electroactive enzymatic product, formed by the HRP-catalyzed reaction with 2-AP–H2O2 substrate solution using a SPE. (C) Typical SWV responses with increasing concentrations of P185-ssDNA, and the resulting calibration plot.
Adapted from Ref. [156] with permission of The Royal Society of Chemistry.

Table 7
CNTs-based electrochemical biosensors for dopamine.

Platform	Detection	Linear range	Detection limit	Sample	Ref.
Si or SiO_2/SWCNTs	FIA Amperometry	0.025–1 μM	0.05 nM	Artificial cerebral spinal fluid	[163]
NbME/MWCNTs	CV	—	11 nM	*In vivo* analysis: anesthetized male rats	[164]
GCE/bMWCNTs	SWV	0.03–55 μM	8.5 nM	Serum and urine	[165]
GCE/aMWCNTs	Amperometry	0.1–1000 μM	30 nM	Artificial sample	[166]
GCE/SWCNTs-PLL	DPV	0.1–2 μM	16 nM	Urine	[168]
Au-MEA/MWCNTs-Naf	SWV	0.0001–1 μM	0.05 nM	Serum	[169]
ITO-MEA/MWCNTs-dsDNA	Amperometry	0.001–10 μM	1 nM	Hippocampal neuronal cultures and hippocampal slices	[170]
GCE/bCNTs-dsDNA	DPV	0.5–7 μM	74 nM	Urine	[171]
GCE/hCNTs-PDDA	DPV	0.25–10 μM	80 nM	Serum	[172]
ITO/MWCNTs-PVI	DPV	0.1–10 μM	40.5 nM	Serum	[173]
CPE/MWCNTs-PEDOT	DPV	0.1–20 μM	20 nM	Artificial mixture	[174]
GCE/PANI/MWCNTs-PSMVM	CV	0.1–1000 μM	50 nM	Artificial mixture	[175]
AuE/MWCNTs-PEI-AuNPs	DPV	0.05–4 μM	6.56 nM	Serum	[176]
GCE/N-MWCNTs-[BMIM][BF_4]	SWV	0.001–40 μM	1 nM	Pharmaceutical sample	[177]
GCE/GO-[BMIM][PF_6]-MWCNTs	SWV	8×10^{-6} to 15μM	3×10^{-3} nM	Artificial mixture	[178]
GCE/MWCNTs-PPy-MIP	DPV	5×10^{-5} to 5 μM	1×10^{-2} nM	Serum and urine	[179]
Gr-CNTs-MIP	CV	2×10^{-9} to 1×10^{-6} μM	6.67×10^{-7} nM	Artificial mixture	[180]
AuE/CA/Tyrosinase/Naf/MWCNTs-Naf	AmperometryDPV	0.05–100 μM1–100 μM	3 nM 50 nM	Pharmaceutical mixtures	[182]
GCE/MWCNTs/$CaCO_3$NPs-Tyrosinase	Amperometry	0.015–30 μM	15 nM	Artificial samples	[183]

Abbreviations: SWCNTs: single-walled carbon nanotubes; FIA: flow injection analysis; NbME: niobium microelectrode; MWCNTs: multi-walled carbon nanotubes; CV: cyclic voltammetry; GCE: glassy carbon electrode; bMWCNTs: oxidized multi-walled carbon nanotubes in basic media; SWV: square wave voltammetry; aMWCNTs: oxidized multi-walled carbon nanotubes in acid media; PLL: polylysine; DPV: differential pulse voltammetry; Au-MEA: gold microelectrode array; ITO-MEA: indium tin oxide microelectrode array; Naf: nafion; dsDNA; double stranded DNA; bCNTs: bamboo-like carbon nanotubes; hCNTs: helical carbon nanotubes; PDDA: poly(diallyldimethylammonium) chloride; PVI: poly(vinyl imidazole); CPE: carbon paste electrode; PEDOT: poly(3,4-ehylenedioxythiophene); PANI: polyaniline; PSMVM: P(St-alt-MAn)-co-P(VM-alt-MAn) copolymer; AuE: gold electrode; PEI: polyethyleneimine; AuNPs: gold nanoparticles; N-MWCNTs: N-doped multi-walled carbon nanotubes; [BMIM][BF_4]: butyl-1-methyl-imidazolium tetrafluorobromate; GO: graphene oxide; [BMIM][PF_6]: 1-butyl-3-methylimidazoulium hexafluorophosphate; PPy: polypyrrole; MIP: molecularly imprinted polymer; Gr: graphene; CNTs: carbon nanotubes; CA: cysteamine; $CaCO_3$NPs: calcium carbonate nanoparticles.

used to functionalize the CNTs allowed an efficient dispersion of the carbon nanostructures and the selective Do quantification in urine samples with a detection limit of 16 nM. Samseya et al. [169] developed a gold microelectrode array (Au-MEA) modified with Nafion-modified MWCNTs. This platform allowed the sensitive (0.05 nM) and selective Do quantification in the presence of ascorbic acid.

The overall conductivity of CNTs and the performance of the resulting Do sensors have been improved by incorporating other conducting materials. For example, Xu et al. [174] prepared a platform based on the electrodeposition of the conducting polymer poly(3,4-ethylenedioxythiophene) (PEDOT) in the presence of MWCNTs at a carbon paste electrode (CPE). The PEDOT-MWCNTs film showed improved electrocatalytic activity toward the oxidation of Do due to the combination of the excellent catalytic properties of both components, allowing the sensitive and selective Do electrochemical sensing. Liu et al. [175] developed an electrochemical Do-sensor based on a GCE modified with PANI and micelle-encapsulated MWCNTs with P(St-alt-Man)-co-P(VM-at-Man) (PSMVM) copolymer (MWCNTs-PSMVM) which presented a wide linear range (0.1–1000 μM). Lin et al. [176] reported a sensor based on the modification of gold with a PEI, MWCNTs, and AuNPs

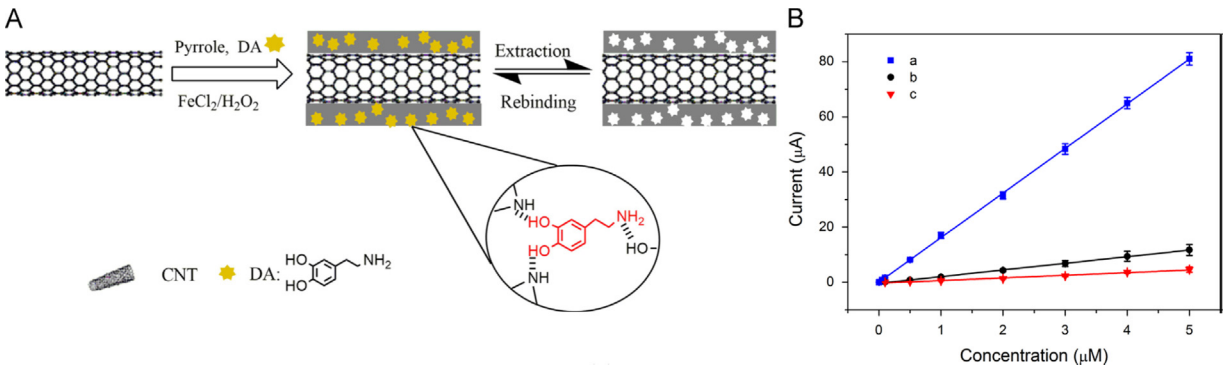

Fig. 9. (A) The chemical route to the preparation of MWCNTs-PPy-MIP. (B) The calibration curve of dopamine obtained with (a) MWCNTs-PPy-MIP, (b) MWCNTs-PPy-NIP, and (c) MWCNTs modified GCE.
Adapted from Ref. [179], Copyright (2014), with permission from Elsevier.

nanocomposite, which presented a detection limit of 6.56 nM and successful application for the determination of Do in serum samples.

Ionic liquids have demonstrated to be suitable modifiers for the preparation of CNT-composite materials with electrochemical sensing applications for Do. Imidazolium-based ionic liquids allowed a successful dispersion of CNTs and the exposure of a 3D functional structure that made possible the fast modification of the nanomaterials without disruption of their conjugated structure. Joshi et al. [177] reported the use of composites based on N-MWCNTs and butyl-1-methyl-imidazolium tetrafluoroborate ([BMIM][BF_4]). The resulting composites made possible the detection of Do at nM levels without interference of ascorbic acid. Wang et al. [178] reported a MWCNTs-GO-1-butyl-3-methylimidazoulium hexafluorophosphate ([BMIM][PF_6]) ionic liquid composite that showed excellent electrochemical properties toward the detection of Do in the presence of a large excess of uric acid and ascorbic acid, with a very low detection limit (3×10^{-3} nM) and wide linear range (8×10^{-6} to 15 μM).

As in the case of the other biomarkers, the use of MIPs offered an interesting alternative for Do quantification. Qian et al. [179] proposed an electrochemical sensor based on the modification of GCE with a MIP synthetized from a mixture of CNTs-pyrrole-$FeCl_2$-Do for *in vivo* detection of Do (Fig. 9). The particular polypyrrole (PPy) structure with plenty cavities allowed the binding of Do through π–π stacking of aromatic rings and hydrogen bonds between the amino groups of Do and the oxygen-containing groups of the polymer (Fig. 9A). Thus, the prepared GCE/MWCNTs-PPy-MIP sensor exhibited high sensitivity and very low detection limit (1×10^{-2} nM) compared to GCE/MWCNTs-PPy-NIP and GCE/MWCNTs (Fig. 9B), indicating the advantages of the MWCNTs-PPy-MIP composite. Li et al. [180] reported the modification of a hybrid graphene foam/CNTs surface with a MIP film (Gr-CNTs-MIP), with an excellent Do performance mainly due to the high surface area of CNTs-3D skeleton and the selectivity and anti-interference capability of MIP film. The detection limit of this Do sensor (6.67×10^{-7} nM) was the lowest obtained from the electrochemical (bio)sensors reported in the period covered by this review.

Tyroninase-based electrochemical sensors are highly selective devices for Do detection. This enzyme catalyzes the oxidation of *o*-diphenols like Do to their respective *o*-quinone derivatives, which in turn are electrochemically reduced back to Do at the electrode surface without any mediator [181]. In this sense, Canbay et al. [182] developed a novel Do biosensor based on a cysteamine/tyrosinase/Nafion/MWCNTs-Nafion composite film-modified Au electrode. The results indicated that (a) the immobilized tyrosinase almost retained its native structure and displayed a high electrocatalytic response of dopamine, and (b) the high porosity and conductivity of the MWCNTs skeleton improved the electrochemical transduction and ensured the easy access of Do to the active site of the enzyme. In fact, this biosensor showed a wide linear amperometric response (0.05–100 μM), a good detection limit (3 nM), high selectivity, and a high operational stability. Cosnier et al. [183] reported the advantages of using $CaCO_3$ nanoparticles ($CaCO_3$NPs) with MWCNTs for the fabrication of a sensitive tyroninase-based Do electrochemical biosensor. $CaCO_3$NPs acted as a biocompatible host matrix for tyrosinase and MWCNTs provided a highly porous conductive skeleton enhancing the enzyme immobilization, ensuring the easy access of Do to the active site of tyrosinase, and improving the electrochemical transduction of enzyme reaction. However, as can be seen in Table 7, the detection limits of these CNTs-Tyrosinase-based detectors are not as good as those obtained with direct electrochemical detection of Do.

5. Conclusions and perspectives

We presented a critical discussion about the most representative CNTs-based electrochemical (bio)sensors for the quantification of biomarkers of clinical relevance reported between 2013 and 2017, emphasizing the advantages of using CNTs in the different steps during the construction of the supramolecular architectures.

The large surface area and the existence of functional groups resulting from the oxidation and/or functionalization of CNTs have demonstrated to play a crucial role as support for the biorecognition elements and the bioconjugates used to amplify the analytical signal. The combination of the unique electronic properties of CNTs, the excellent electrochemical activity of their edge-plane like defects, the advantages inherent to the affinity and enzymatic recognition, catalysis, and direct charge transfer, made possible the development of a large number of (bio)sensing schemes for the highly sensitive and selective quantification of biomarkers. Particularly, the variety of affinity interactions used in the different approaches: antigen-antibody, aptamer-complementary DNA sequence/target, peptide-target, DNA-miRNA, protein-dsRNA, DNA-DNA, MIP-target, host–guest, allowed the development of a long list of bioanalytical platforms with different schemes for the transduction of the biorecognition event and the generation the analytical signal.

In spite of the clear success of CNTs-based electrochemical (bio)sensors for biomarkers, there are still some requirements of the medicine and clinical chemistry of XXI-century that need to be addressed. The development of miniaturized, non-invasive, fast, simple, and efficient devices able to be used for point-of-care (POC) measurements is one of the most urgent challenges. Therefore, in

addition to sensitivity and selectivity, the robustness and long-term stability of the (bio)sensors are very important aspects to be considered for future devices. In this sense, the incorporation of aptamers, peptides, and MIPs represents a new and promising alternative due to the advantages inherent to these (bio)recognition molecules. Another aspect important to remark is that, even when the signal amplification with secondary antibodies/markers have demonstrated high efficiency, one-step (label free) biosensing schemes should be highly recommended for sensitive, selective, fast, and simple-to-operate POC devices. Another important challenge is the development of multi-target platforms to allow the simultaneous quantification of different biomarkers in the same sample. As it was previously illustrated, at present there are some interesting attempts although the validation with a large number of patient samples is still required.

No less important is the careful control of the CNTs synthesis, especially connected with their chirality and density/type of defects. This is a key aspect to ensure high efficiency in the mass-production of CNTs-based biosensors and reproducibility in the analytical performance. The knowledge of the toxicity of CNTs is another aspect that have started receiving great attention in the last years mainly due to possible *in vivo* applications and the effect on the environment.

As final consideration, it is important to remark that, while carbon nanotubes and graphene derivatives have been the most widely used carbon nanoallotropes for the construction of biomarkers electrochemical biosensors; in the last years, carbon nanohorns, carbon dots, and nanohybrids based on the combination of carbon nanoallotropes have started to receive increasing attention due to their unique characteristics. It is expected that the knowledge of basic aspects of these supramolecular architectures based on the combination of multiple basic carbon nanoallotropes or the decoration of the outer surface of carbon nanotubes and graphene with other nanoallotropes will revolutionize the field of biomarkers electrochemical (bio)sensors.

Acknowledgements

Gustavo Rivas, Marcela Rodríguez, and Concepción Parrado wish to express our deepest gratitude to Prof. Wang for his valuable contributions to our scientific careers. We were fortunate to have such unique and famous TEACHER during our postdoc time. In fact, at Dr. Wang's laboratory, we not only learned about biosensors and electroanalytical chemistry, we also learned how to be successful with every daily scientific challenge, how to manage a big group, and how to write very innovative projects. Dr. Wang has also given us an incredible example: even reaching high positions, being very famous and having hundreds of papers, is necessary to work everyday as hard as the first one. In addition, and even more important, is the warm friendship of Dr. Wang kept over the years.

Dr. Wang. . . Many many thanks and happy birthday!

The authors are grateful to CONICET, ANPCyT, and SECyT-UNC for the financial support of the research activities. E.N.P., C.T., M.L.R., and P.G. acknowledge CONICET and A.M. thanks ANPCyT for the fellowships received.

References

[1] A. Zhang, C.M. Lieber, Nano-bioelectronics, Chem. Rev. 116 (2016) 215–257.
[2] X. Zhu, J. Li, H. He, M. Huang, X. Zhang, S. Wang, Application of nanomaterials in the bioanalytical detection of disease-related genes, Biosens. Bioelectron. 74 (2015) 113–133.
[3] L. Syedmoradi, M. Daneshpour, M. Alvandipour, F.A. Gomez, H. Hajghassem, K. Omidfar, Point of care testing: the impact of nanotechnology, Biosens. Bioelectron. 87 (2017) 373–387.
[4] P.J. Britto, K.S.V. Santhanam, P.M. Ajayan, Carbon nanotube electrode for oxidation of dopamine, Bioelectrochem. Bioenerg. 41 (1996) 121–125.
[5] J.N. Tiwari, V. Vij, K.C. Kemp, K.S. Kim, Engineered carbon-nanomaterial-based electrochemical sensors for biomolecules, ACS Nano 10 (2016) 46–80.
[6] N. Yang, G.M. Swain, X. Jiang, Nanocarbon electrochemistry and electroanalysis: current status and future perspectives, Electroanalysis 28 (2016) 27–34.
[7] Z. Wang, Z. Dai, Carbon nanomaterials-based electrochemical biosensors: an overview, Nanoscale 7 (2015) 6420–6431.
[8] S. Sánchez, M. Pumera, E. Cabruja, E. Fàbregas, Carbon nanotube/polysulfone composite screen-printed electrochemical enzyme biosensors, Analyst 132 (2007) 142–147.
[9] T. Feng, Y. Wang, X. Qiao, Recent advances of carbon nanotubes-based electrochemical immunosensors for the detection of protein cancer biomarkers, Electroanalysis 29 (2017) 662–675.
[10] M.S. Dresselhaus, G. Dresselhaus, A. Jorio, Unusual properties and structure of carbon nanotubes, Annu. Rev. Mater. Res. 34 (2004) 247–278.
[11] E.N. Primo, F. Gutierrez, M.D. Rubianes, N.F. Ferreyra, M.C. Rodríguez, M.L. Pedano, A. Gasnier, A. Gutierrez, M. Eguílaz, P. Dalmasso, G. Luque, S. Bollo, C. Parrado, G.A. Rivas, Electrochemistry in one dimension: applications of carbon nanotubes, in: R.C. Alkire, P.N. Bartlett, J. Lipkowski (Eds.), Electrochemistry of Carbon Electrodes, Wiley-VCH Verlag GmbH & Co. KGaA, Weinheim, 2015, pp. 83–119.
[12] V. Georgakilas, J.A. Perman, J. Tucek, R. Zboril, Broad family of carbon nanoallotropes: classification, chemistry, and applications of fullerenes, carbon dots, nanotubes, graphene, nanodiamonds, and combined superstructures, Chem. Rev. 115 (2015) 4744–4822.
[13] Z. Li, Z. Liu, H. Sun, C. Gao, Superstructured assembly of nanocarbons: fullerenes, nanotubes, and graphene, Chem. Rev. 115 (2015) 7046–7177.
[14] L. Wang, M. Pumera, Electrochemical catalysis at low dimensional carbons: graphene, carbon nanotubes and beyond – a review, Appl. Mater. Today 5 (2016) 134–141.
[15] M. Pumera, The electrochemistry of carbon nanotubes: fundamentals and applications, Chem. Eur. J. 15 (2009) 4970–4978.
[16] L. Kong, W. Chen, Carbon nanotube and graphene-based bioinspired electrochemical actuators, Adv. Mater. 26 (2014) 1025–1043.
[17] P. Yáñez-Sedeño, A. González-Cortés, L. Agüí, J.M. Pingarrón, Uncommon carbon nanostructures for the preparation of electrochemical immunosensors, Electroanalysis 28 (2016) 1679–1691.
[18] C. Gao, Z. Guo, J.-H. Liu, X.-J. Huang, The new age of carbon nanotubes: an updated review of functionalized carbon nanotubes in electrochemical sensors, Nanoscale 4 (2012) 1948–1963.
[19] S.W. Kim, T. Kim, Y.S. Kim, H.S. Choi, H.J. Lim, S.J. Yang, C.R. Park, Surface modifications for the effective dispersion of carbon nanotubes in solvents and polymers, Carbon 50 (2012) 3–33.
[20] E.N. Primo, F.A. Gutierrez, G.L. Luque, P.R. Dalmasso, A. Gasnier, Y. Jalit, M. Moreno, M.V. Bracamonte, M.E. Rubio, M.L. Pedano, M.C. Rodríguez, N.F. Ferreyra, M.D. Rubianes, S. Bollo, G.A. Rivas, Comparative study of the electrochemical behavior and analytical applications of (bio)sensing platforms based on the use of multi-walled carbon nanotubes dispersed in different polymers, Anal. Chim. Acta 805 (2013) 19–35.
[21] D. Baskaran, J.W. Mays, M.S. Bratcher, Noncovalent and nonspecific molecular interactions of polymers with multiwalled carbon nanotubes, Chem. Mater. 17 (2005) 3389–3397.
[22] M. Eguílaz, C.J. Venegas, A. Gutiérrez, G.A. Rivas, S. Bollo, Carbon nanotubes non-covalently functionalized with cytochrome c: a new bioanalytical platform for building bienzymatic biosensors, Microchem. J. 128 (2016) 161–165.
[23] M. Eguílaz, A. Gutiérrez, F. Gutierrez, J.M. González-Domínguez, A. Ansón-Casaos, J. Hernández-Ferrer, N.F. Ferreyra, M.T. Martínez, G. Rivas, Covalent functionalization of single-walled carbon nanotubes with polytyrosine: characterization and analytical applications for the sensitive quantification of polyphenols, Anal. Chim. Acta 909 (2016) 51–59.
[24] F.A. Gutierrez, J.M. González-Domínguez, A. Ansón-Casaos, J. Hernández-Ferrer, M.D. Rubianes, M.T. Martínez, G. Rivas, Single-walled carbon nanotubes covalently functionalized with cysteine: a new alternative for the highly sensitive and selective Cd(II) quantification, Sens. Actuators B: Chem. 249 (2017) 506–514.
[25] Biomarkers and surrogate endpoints: preferred definitions and conceptual framework, Clin. Pharmacol. Ther. 69 (2001) 89–95.
[26] N.J. Ronkainen, S.L. Okon, Nanomaterial-based electrochemical immunosensors for clinically significant biomarkers, Materials 7 (2014) 4669–4709.
[27] S. Campuzano, P. Yáñez-Sedeño, J.M. Pingarrón, Electrochemical genosensing of circulating biomarkers, Sensors 17 (2017) 866–885.
[28] Y. Wang, X. Li, W. Cao, Y. Li, H. Li, B. Du, Q. Wei, Ultrasensitive sandwich-type electrochemical immunosensor based on a novel signal amplification strategy using highly loaded toluidine blue/gold nanoparticles decorated KIT-6/carboxymethyl chitosan/ionic liquids as signal labels, Biosens. Bioelectron. 61 (2014) 618–624.
[29] S. Hammarström, E. Engvall, B.G. Johansson, S. Svensson, G. Sundblad, I.J. Goldstein, Nature of the tumor-associated determinant(s) of carcinoembryonic antigen, Proc. Natl. Acad. Sci. U.S.A. 72 (1975) 1528–1532.
[30] M.G. Fakih, A. Padmanabhan, CEA monitoring in colorectal cancer. What you should know, Oncol. 20 (2006) 579–587.

[31] A.M. Ballesta, R. Molina, X. Filella, J. Jo, N. Giménez, Carcinoembryonic antigen in staging and follow-up of patients with solid tumors, Tumor Biol. 16 (1995) 32–41.
[32] F. Naghibalhossaini, P. Ebadi, Evidence for CEA release from human colon cancer cells by an endogenous GPI-PLD enzyme, Cancer Lett. 234 (2006) 158–167.
[33] M. Hasanzadeh, N. Shadjou, Advanced nanomaterials for use in electrochemical and optical immunoassays of carcinoembryonic antigen. A review, Microchim. Acta 184 (2017) 389–414.
[34] F. Li, L. Jiang, J. Han, Q. Liu, Y. Dong, Y. Li, Q. Wei, A label-free amperometric immunosensor for the detection of carcinoembryonic antigen based on novel magnetic carbon and gold nanocomposites, RSC Adv. 5 (2015) 19961–19969.
[35] X. Pang, J. Li, Y. Zhao, D. Wu, Y. Zhang, B. Du, H. Ma, Q. Wei, Label-free electrochemiluminescent immunosensor for detection of carcinoembryonic antigen based on nanocomposites of GO/MWCNTs-COOH/Au@CeO2, ACS Appl. Mater. Interfaces 7 (2015) 19260–19267.
[36] D. Feng, L. Li, X. Fang, X. Han, Y. Zhang, Dual signal amplification of horseradish peroxidase functionalized nanocomposite as trace label for the electrochemical detection of carcinoembryonic antigen, Electrochim. Acta 127 (2014) 334–341.
[37] J. Han, Y. Li, J. Feng, M. Li, P. Wang, Z. Chen, Y. Dong, A novel sandwich-type immunosensor for detection of carcino-embryonic antigen using silver hybrid multiwalled carbon nanotubes/manganese dioxide, J. Electroanal. Chem. 786 (2017) 112–119.
[38] Z. Yan, H. Ma, D. Fan, L. Hu, X. Pang, J. Gao, Q. Wei, Q. Wang, An ultrasensitive sandwich-type electrochemical immunosensor for carcino embryonie antigen based on supermolecular labeling strategy, J. Electroanal. Chem. 781 (2016) 289–295.
[39] N. Li, Y. Wang, W. Cao, Y. Zhang, T. Yan, B. Du, Q. Wei, An ultrasensitive electrochemical immunosensor for CEA using MWCNT-NH_2 supported PdPt nanocages as labels for signal amplification, J. Mater. Chem. B 3 (2015) 2006–2011.
[40] J. Han, L. Jiang, F. Li, P. Wang, Q. Liu, Y. Dong, Y. Li, Ultrasensitive non-enzymatic immunosensor for carcino-embryonic antigen based on palladium hybrid vanadium pentoxide/multiwalled carbon nanotubes, Biosens. Bioelectron. 77 (2016) 1104–1111.
[41] T. Ross, K. Ahmed, N. Raison, B. Challacombe, P. Dasgupta, Clarifying the PSA grey zone: the management of patients with a borderline PSA, Int. J. Clin. Pract. 70 (2016) 950–959.
[42] J. Peng, Y. Di Zhu, X.H. Li, L.P. Jiang, E.S. Abdel-Halim, J.J. Zhu, Electrochemical immunoassay for the prostate specific antigen using ceria mesoporous nanospheres, Microchim. Acta 181 (2014) 1505–1512.
[43] B. Kavosi, A. Salimi, R. Hallaj, K. Amani, A highly sensitive prostate-specific antigen immunosensor based on gold nanoparticles/PAMAM dendrimer loaded on MWCNTS/chitosan/ionic liquid nanocomposite, Biosens. Bioelectron. 52 (2014) 20–28.
[44] A. Salimi, B. Kavosi, F. Fathi, R. Hallaj, Highly sensitive immunosensing of prostate-specific antigen based on ionic liquid–carbon nanotubes modified electrode: application as cancer biomarker for prostate biopsies, Biosens. Bioelectron. 42 (2013) 439–446.
[45] J. Yang, W. Wen, X. Zhang, S. Wang, Electrochemical immunosensor for the prostate specific antigen detection based on carbon nanotube and gold nanoparticle amplification strategy, Microchim. Acta 182 (2015) 1855–1861.
[46] X. Qin, A. Xu, L. Liu, W. Deng, C. Chen, Y. Tan, Y. Fu, Q. Xie, S. Yao, Ultrasensitive electrochemical immunoassay of proteins based on *in situ* duple amplification of gold nanoparticle biolabel signals, Chem. Commun. 51 (2015) 8540–8543.
[47] Y. Liu, Y. Zhao, Z. Zhu, Z. Xing, H. Ma, Q. Wei, Ultrasensitive immunosensor for prostate specific antigen using biomimetic polydopamine nanospheres as an electrochemiluminescence superquencher and antibody carriers, Anal. Chim. Acta 963 (2017) 17–23.
[48] Y. He, Y. Chai, R. Yuan, H. Wang, L. Bai, N. Liao, A supersandwich electrochemiluminescence immunosensor based on mimic-intramolecular interaction for sensitive detection of proteins, Analyst 139 (2014) 5209–5214.
[49] F. Liu, W. Deng, Y. Zhang, S. Ge, J. Yu, X. Song, Application of ZnO quantum dots dotted carbon nanotube for sensitive electrochemiluminescence immunoassay based on simply electrochemical reduced Pt/Au alloy and a disposable device, Anal. Chim. Acta 818 (2014) 46–53.
[50] L. Tian, L. Liu, Y. Li, Q. Wei, W. Cao, 3D sandwich-type prostate specific antigen (PSA) immunosensor based on rGO–MWCNT–Pd nanocomposite, New J. Chem. 39 (2015) 5522–5528.
[51] L. Liu, Y. Li, L. Tian, Q. Wei, W. Cao, Ultrasensitive sandwich-type prostate specific antigen immunosensor based on Ag overgrowth in Pd nano-octahedrons heterodimers decorated on amino functionalized multiwalled carbon nanotubes, Sens. Actuators B: Chem. 237 (2016) 733–739.
[52] B. Zhang, Y. He, B. Liu, D. Tang, NiCoBP-doped carbon nanotube hybrid: a novel oxidase mimetic system for highly efficient electrochemical immunoassay, Anal. Chim. Acta 851 (2014) 49–56.
[53] Y. He, S. Xie, X. Yang, R. Yuan, Y. Chai, Electrochemical peptide biosensor based on *in situ* silver deposition for detection of prostate specific antigen, ACS Appl. Mater. Interfaces 7 (2015) 13360–13366.
[54] M.S. Wu, R.N. Chen, Y. Xiao, Z.X. Lv, Novel "signal-on" electrochemiluminescence biosensor for the detection of PSA based on resonance energy transfer, Talanta 161 (2016) 271–277.
[55] F. Tahmasebi, A. Noorbakhsh, Sensitive electrochemical prostate specific antigen aptasensor: effect of carboxylic acid functionalized carbon nanotube and glutaraldehyde linker, Electroanalysis 28 (2016) 1134–1145.
[56] E. Heydari-Bafrooei, N.S. Shamszadeh, Electrochemical bioassay development for ultrasensitive aptasensing of prostate specific antigen, Biosens. Bioelectron. 91 (2017) 284–292.
[57] S. Patra, E. Roy, R. Madhuri, P.K. Sharma, Nano-iniferter based imprinted sensor for ultra trace level detection of prostate-specific antigen in both men and women, Biosens. Bioelectron. 66 (2015) 1–10.
[58] N. Li, H. Ma, W. Cao, D. Wu, T. Yan, B. Du, Q. Wei, Highly sensitive electrochemical immunosensor for the detection of alpha fetoprotein based on PdNi nanoparticles and N-doped graphene nanoribbons, Biosens. Bioelectron. 74 (2015) 786–791.
[59] Q. Gao, J. Han, Z. Ma, Polyamidoamine dendrimers-capped carbon dots/Au nanocrystal nanocomposites and its application for electrochemical immunosensor, Biosens. Bioelectron. 49 (2013) 323–328.
[60] S. Sharma, R. Raghav, R. O'Kennedy, S. Srivastava, Advances in ovarian cancer diagnosis: a journey from immunoassays to immunosensors, Enzyme Microb. Technol. 89 (2016) 15–30.
[61] C.I.L. Justino, A.C. Duarte, T.A.P. Rocha-Santos, Critical overview on the application of sensors and biosensors for clinical analysis, TrAC Trends Anal. Chem. 85 (2016) 36–60.
[62] J. Guo, X. Han, J. Wang, J. Zhao, Z. Guo, Y. Zhang, Horseradish peroxidase functionalized gold nanorods as a label for sensitive electrochemical detection of alpha-fetoprotein antigen, Anal. Biochem. 491 (2015) 58–64.
[63] H. Wang, H. Li, Y. Zhang, Q. Wei, H. Ma, D. Wu, Y. Li, Y. Zhang, B. Du, Label-free immunosensor based on Pd nanoplates for amperometric immunoassay of alpha-fetoprotein, Biosens. Bioelectron. 53 (2014) 305–309.
[64] J. Gao, H. Ma, X. Lv, T. Yan, N. Li, W. Cao, Q. Wei, A novel electrochemical immunosensor using β-cyclodextrins functionalized silver supported adamantine-modified glucose oxidase as labels for ultrasensitive detection of alpha-fetoprotein, Anal. Chim. Acta 893 (2015) 49–56.
[65] B. Zhao, J. Yan, D. Wang, Z. Ge, S. He, D. He, S. Song, C. Fan, Carbon nanotubes multifunctionalized by rolling circle amplification and their application for highly sensitive detection of cancer markers, Small 9 (2013) 2595–2601.
[66] K. Muzyka, Current trends in the development of the electrochemiluminescent immunosensors, Biosens. Bioelectron. 54 (2014) 393–407.
[67] B. Piro, S. Reisberg, Recent advances in electrochemical immunosensors, Sensors (Switzerland) 17 (2017) 794–856.
[68] H. Yang, Z. Li, X. Wei, R. Huang, H. Qi, Q. Gao, C. Li, C. Zhang, Detection and discrimination of alpha-fetoprotein with a label-free electrochemical impedance spectroscopy biosensor array based on lectin functionalized carbon nanotubes, Talanta 111 (2013) 62–68.
[69] J. Lin, Z. Wei, H. Zhang, M. Shao, Sensitive immunosensor for the label-free determination of tumor marker based on carbon nanotubes/mesoporous silica and graphene modified electrode, Biosens. Bioelectron. 41 (2013) 342–347.
[70] Y. Wang, Y. Qu, X.X. Ye, K. Wu, C. Li, Fabrication of an electrochemical immunosensor for α-fetoprotein based on a poly-L-lysine-single-walled carbon nanotubes/Prussian blue composite film interface, J. Solid State Electrochem. 20 (2016) 2217–2222.
[71] L. Jiao, Z. Mu, C. Zhu, Q. Wei, H. Li, D. Du, Y. Lin, Chemical graphene loaded bimetallic Au@Pt nanodendrites enhancing ultrasensitive electrochemical immunoassay of AFP, Sens. Actuators B: Chem. 231 (2016) 513–519.
[72] L. Ji, Z. Guo, T. Yan, H. Ma, B. Du, Y. Li, Q. Wei, Ultrasensitive sandwich-type electrochemical immunosensor based on a novel signal amplification strategy using highly loaded palladium nanoparticles/carbon decorated magnetic microspheres as signal labels, Biosens. Bioelectron. 68 (2015) 757–762.
[73] F. Li, J. Han, L. Jiang, Y. Wang, Y. Li, Y. Dong, Q. Wei, An ultrasensitive sandwich-type electrochemical immunosensor based on signal amplification strategy of gold nanoparticles functionalized magnetic multi-walled carbon nanotubes loaded with lead ions, Biosens. Bioelectron. 68 (2015) 626–632.
[74] L. Jiang, J. Han, F. Li, J. Gao, Y. Li, Y. Dong, Q. Wei, A sandwich-type electrochemical immunosensor based on multiple signal amplification for α-fetoprotein labeled by platinum hybrid multiwalled carbon nanotubes adhered copper oxide, Electrochim. Acta 160 (2015) 7–14.
[75] F. Yang, Y. Chai, R. Yuan, J. Han, Y. Yuan, N. Liao, Z. Yang, Ultrasensitive electrochemical immunosensors for clinical immunoassay using gold nanoparticle coated multi-walled carbon nanotubes as labels and horseradish peroxidase as an enhancer, Anal. Methods 5 (2013) 5279–5285.
[76] D. Feng, L. Li, J. Zhao, Y. Zhang, Simultaneous electrochemical detection of multiple biomarkers using gold nanoparticles decorated MWCNTs as signal enhancers, Anal. Biochem. 482 (2015) 48–54.
[77] H. Niu, R. Yuan, Y. Chai, L. Mao, H. Liu, Y. Cao, Highly amplified electrochemiluminescence of peroxydisulfate using bienzyme functionalized palladium nanoparticles as labels for ultrasensitive immunoassay, Biosens. Bioelectron. 39 (2013) 296–299.
[78] H. Dai, G. Xu, S. Zhang, L. Gong, X. Li, C. Yang, Y. Lin, J. Chen, G. Chen, Carbon nanotubes functionalized electrospun nanofibers formed 3D electrode

enables highly strong ECL of peroxydisulfate and its application in immunoassay, Biosens. Bioelectron. 61 (2014) 575–578.
[79] I. Raphael, S. Nalawade, T.N. Eagar, T.G. Forsthuber, T cell subsets and their signature cytokines in autoimmune and inflammatory diseases, Cytokine 74 (2015) 5–17.
[80] C. Blandizzi, P. Gionchetti, A. Armuzzi, R. Caporali, S. Chimenti, R. Cimaz, L. Cimino, G. Lapadula, P. Lionetti, A. Marchesoni, A. Marcellusi, F.S. Mennini, C. Salvarani, G. Girolomoni, The role of tumour necrosis factor in the pathogenesis of immune-mediated diseases, Int. J. Immunopathol. Pharmacol. 27 (2014) 1–10.
[81] M. Mazloum-Ardakani, L. Hosseinzadeh, A. Khoshroo, Label-free electrochemical immunosensor for detection of tumor necrosis factor α based on fullerene-functionalized carbon nanotubes/ionic liquid, J. Electroanal. Chem. 757 (2015) 58–64.
[82] M. Mazloum-Ardakani, L. Hosseinzadeh, Highly-sensitive label-free immunosensor for tumor necrosis factor α based on Ag@Pt core–shell nanoparticles supported on MWCNTs as an efficient electrocatalyst nanocomposite, RSC Adv. 5 (2015) 70781–70786.
[83] M. Mazloum-Ardakani, L. Hosseinzadeh, A. Khoshroo, Ultrasensitive electrochemical immunosensor for detection of tumor necrosis factor-α based on functionalized MWCNT-gold nanoparticle/ionic liquid nanocomposite, Electroanalysis 27 (2015) 2518–2526.
[84] M. Ebrahimi-Mamaeghani, S. Mohammadi, S.R. Arefhosseini, P. Fallah, Z. Bazi, Adiponectin as a potential biomarker of vascular disease, Vasc. Health Risk Manag. 11 (2015) 55–70.
[85] I. Ojeda, M. Barrejón, L.M. Arellano, A. González-Cortés, P. Yáñez-Sedeño, F. Langa, J.M. Pingarrón, Grafted-double walled carbon nanotubes as electrochemical platforms for immobilization of antibodies using a metallic-complex chelating polymer: application to the determination of adiponectin cytokine in serum, Biosens. Bioelectron. 74 (2015) 24–29.
[86] G. Wang, X. He, L. Chen, Y. Zhu, X. Zhang, Ultrasensitive IL-6 electrochemical immunosensor based on Au nanoparticles-graphene-silica biointerface, Colloids Surf. B: Biointerfaces 116 (2014) 714–719.
[87] T. Yang, S. Wang, H. Jin, W. Bao, S. Huang, J. Wang, An electrochemical impedance sensor for the label-free ultrasensitive detection of interleukin-6 antigen, Sens. Actuators B: Chem. 178 (2013) 310–315.
[88] N.P. Sardesai, K. Kadimisetty, R. Faria, J.F. Rusling, A microfluidic electrochemiluminescent device for detecting cancer biomarker proteins, Anal. Bioanal. Chem. 405 (2013) 3831–3838.
[89] K. Kadimisetty, S. Malla, N.P. Sardesai, A.A. Joshi, R.C. Faria, N.H. Lee, J.F. Rusling, Automated multiplexed ECL immunoarrays for cancer biomarker proteins, Anal. Chem. 87 (2015) 4472–4478.
[90] E. Sánchez-Tirado, C. Salvo, A. González-Cortés, P. Yáñez-Sedeño, F. Langa, J.M. Pingarrón, Electrochemical immunosensor for simultaneous determination of interleukin-1 beta and tumor necrosis factor alpha in serum and saliva using dual screen printed electrodes modified with functionalized double-walled carbon nanotubes, Anal. Chim. Acta 959 (2017) 66–73.
[91] S. Lee, R. Chan, J. Wu, H. Chen, S. Chang, C. Lee, Diagnostic value of procalcitonin for bacterial infection in elderly patients – a systemic review and meta-analysis, Int. J. Clin. Pract. 67 (2013) 1350–1357.
[92] P. Li, W. Zhang, X. Zhou, L. Zhang, C60 carboxyfullerene-based functionalised nanohybrids as signal-amplifying tags for the ultrasensitive electrochemical detection of procalcitonin, Clin. Biochem. 48 (2015) 156–161.
[93] Z.H. Yang, Y. Zhuo, R. Yuan, Y.Q. Chai, Electrochemical activity and electrocatalytic property of cobalt phthalocyanine nanoparticles-based immunosensor for sensitive detection of procalcitonin, Sensor. Actuators B: Chem. 227 (2016) 212–219.
[94] F. Liu, G. Xiang, R. Yuan, X. Chen, F. Luo, D. Jiang, S. Huang, Y. Li, X. Pu, Procalcitonin sensitive detection based on graphene-gold nanocomposite film sensor platform and single-walled carbon nanohorns/hollow Pt chains complex as signal tags, Biosens. Bioelectron. 60 (2014) 210–217.
[95] Y.S. Fang, H.Y. Wang, L.S. Wang, J.F. Wang, Electrochemical immunoassay for procalcitonin antigen detection based on signal amplification strategy of multiple nanocomposites, Biosens. Bioelectron. 51 (2014) 310–316.
[96] V.L. Roger, A.S. Go, D.M. Lloyd-Jones, E.J. Benjamin, J.D. Berry, W.B. Borden, D.M. Bravata, S. Dai, E.S. Ford, C.S. Fox, H.J. Fullerton, C. Gillespie, S.M. Hailpern, J.A. Heit, V.J. Howard, B.M. Kissela, S.J. Kittner, D.T. Lackland, J.H. Lichtman, L.D. Lisabeth, D.M. Makuc, G.M. Marcus, A. Marelli, D.B. Matchar, C.S. Moy, D. Mozaffarian, M.E. Mussolino, G. Nichol, N.P. Paynter, E.Z. Soliman, P.D. Sorlie, N. Sotoodehnia, T.N. Turan, S.S. Virani, N.D. Wong, D. Woo, M.B. Turner, Heart disease and stroke statistics—2012 update, Circulation 125 (2012), e2 LP-e220.
[97] Z. Yang, D. Min Zhou, Cardiac markers and their point-of-care testing for diagnosis of acute myocardial infarction, Clin. Biochem. 39 (2006) 771–780.
[98] M. Hasanzadeh, N. Shadjou, M. Eskandani, M. de la Guardia, E. Omidinia, Electrochemical nano-immunosensing of effective cardiac biomarkers for acute myocardial infarction, TrAC Trends Anal. Chem. 49 (2013) 20–30.
[99] S.J. Aldous, Cardiac biomarkers in acute myocardial infarction, Int. J. Cardiol. 164 (2013) 282–294.
[100] V. Singh, P. Martinezclark, M. Pascual, E.S. Shaw, W.W. O'Neill, Cardiac biomarkers – the old and the new: a review, Coron. Artery Dis. 21 (2010) 244–256.
[101] W. Brian Gibler, G.P. Young, J.R. Hedges, L.M. Lewis, M.S. Smith, S.C. Carleton, R.V. Aghababian, R.O. Jorden, E. Jackson Allison Jr., E.J. Often, P.K. Makens, C. Hamilton, Acute myocardial infarction in chest pain patients with nondiagnostic ECGs: serial CK-MB sampling in the emergency department, Ann. Emerg. Med. 21 (1992) 504–512.
[102] F.T.C. Moreira, R.A.F. Dutra, J.P. Noronha, M.G.F. Sales, Novel sensory surface for creatine kinase electrochemical detection, Biosens. Bioelectron. 56 (2014) 217–222.
[103] P. Garg, P. Morris, A.L. Fazlanie, S. Vijayan, B. Dancso, A.G. Dastidar, S. Plein, C. Mueller, P. Haaf, Cardiac biomarkers of acute coronary syndrome: from history to high-sensitivity cardiac troponin, Intern. Emerg. Med. 12 (2017) 147–155.
[104] S. Agewall, E. Giannitsis, T. Jernberg, H. Katus, Troponin elevation in coronary vs. non-coronary disease, Eur. Heart J. 32 (2011) 404–411.
[105] B.V.M. Silva, I.T. Cavalcanti, M.M.S. Silva, R.F. Dutra, A carbon nanotube screen-printed electrode for label-free detection of the human cardiac troponin T, Talanta 117 (2013) 431–437.
[106] S.L.R. Gomes-Filho, A.C.M.S. Dias, M.M.S. Silva, B.V.M. Silva, R.F. Dutra, A carbon nanotube-based electrochemical immunosensor for cardiac troponin T, Microchem. J. 109 (2013) 10–15.
[107] S. Singal, A.K. Srivastava, S. Dhakate, A.M. Biradar, Electroactive graphene-multi-walled carbon nanotube hybrid supported impedimetric immunosensor for the detection of human cardiac troponin-I, RSC Adv. 5 (2015) 74994–75003.
[108] S. Singal, A.K. Srivastava, B. Gahtori, Rajesh, Immunoassay for troponin I using a glassy carbon electrode modified with a hybrid film consisting of graphene and multiwalled carbon nanotubes and decorated with platinum nanoparticles, Microchim. Acta 183 (2016) 1375–1384.
[109] M.D. Prakash, S.G. Singh, C.S. Sharma, V.S.R. Krishna, Electrochemical detection of cardiac biomarkers utilizing electrospun multiwalled carbon nanotubes embedded SU-8 nanofibers, Electroanalysis 29 (2017) 380–386.
[110] V. Kumar, M. Shorie, A.K. Ganguli, P. Sabherwal, Graphene-CNT nanohybrid aptasensor for label free detection of cardiac biomarker myoglobin, Biosens. Bioelectron. 72 (2015) 56–60.
[111] Y. Ma, X.-L. Shen, H.-S. Wang, J. Tao, J.-Z. Huang, Q. Zeng, L.-S. Wang, MIPs-graphene nanoplatelets-MWCNTs modified glassy carbon electrode for the determination of cardiac troponin I, Anal. Biochem. 520 (2017) 9–15.
[112] V. Serafín, L. Agüí, P. Yáñez-Sedeño, J.M. Pingarrón, Electrochemical immunosensor for the determination of insulin-like growth factor-1 using electrodes modified with carbon nanotubes-poly(pyrrole propionic acid) hybrids, Biosens. Bioelectron. 52 (2014) 98–104.
[113] A.F. Swindall, A. Londoño-Joshi, M. Schultz, N. Fineberg, D. Buchsbaum, S. Bellis, ST6Gal-I protein expression is upregulated in human epithelial tumors and correlates with stem cell markers in normal tissues and colon cancer cell lines, Cancer Res. 73 (2013) 2368–2378.
[114] J. Zhang, J. He, W. Xu, L. Gao, Y. Guo, W. Li, C. Yu, A novel immunosensor for detection of beta-galactoside alpha-2, 6-sialyltransferase in serum based on gold nanoparticles loaded on Prussian blue-based hybrid nanocomposite film, Electrochim. Acta 156 (2015) 45–52.
[115] R.C. Lee, The *C. elegans* heterochronic gene lin-4 encodes small RNAs with antisense complementarity to lin-14, Cell 75 (1993) 843–854.
[116] G.G. Jayaraj, S. Nahar, S. Maiti, Nonconventional chemical inhibitors of microRNA: therapeutic scope, Chem. Commun. 51 (2015) 820–831.
[117] R.C. Friedman, K.K.H. Farh, C.B. Burge, D.P. Bartel, Most mammalian mRNAs are conserved targets of microRNAs, Genome Res. 19 (2009) 92–105.
[118] C.C. Pritchard, H.H. Cheng, M. Tewari, MicroRNA profiling: approaches and considerations, Nat. Rev. Genet. 13 (2012) 358–369.
[119] D.P. Bartel, MicroRNAs: target recognition and regulatory functions, Cell 136 (2009) 215–233.
[120] N. Stoicea, A. Du, C.D. Lakis, C. Tipton, C.E. Arias-Morales, S.D. Bergese, The miRNA journey from theory to practice as a CNS biomarker, Front. Genet. 7 (2016) 1–8.
[121] I. Faravelli, S. Corti, MicroRNA-directed neuronal reprogramming as a therapeutic strategy for neurological diseases, Mol. Neurobiol. (2017).
[122] M.R. Ashoori, M. Rahmati-Yamchi, A. Ostadrahimi, S. Fekri Aval, N. Zarghami, MicroRNAs and adipocytokines: promising biomarkers for pharmacological targets in diabetes mellitus and its complications, Biomed. Pharmacother. 93 (2017) 1326–1336.
[123] I.V. Snowhite, G. Allende, J. Sosenko, R.L. Pastori, S. Messinger Cayetano, A. Pugliese, Association of serum microRNAs with islet autoimmunity, disease progression and metabolic impairment in relatives at risk of type 1 diabetes, Diabetologia 60 (2017) 1409–1422.
[124] J.C. Hongjian Wang, The role of microRNAs in in heart failure, Biochim. Biophys. Acta 1863 (2017) 2019–2030.
[125] E.L. Vegter, E.S. Ovchinnikova, D.J. van Veldhuisen, T. Jaarsma, E. Berezikov, P. van der Meer, A.A. Voors, Low circulating microRNA levels in heart failure patients are associated with atherosclerotic disease and cardiovascular-related rehospitalizations, Clin. Res. Cardiol. 106 (2017) 1–12.
[126] K. Kashani, W. Cheungpasitporn, C. Ronco, Biomarkers of acute kidney injury: the pathway from discovery to clinical adoption, Clin. Chem. Lab. Med. 55 (2017) 1074–1089.
[127] J.X. Xie, X. Fan, C.A. Drummond, R. Majumder, Y. Xie, T. Chen, L. Liu, S.T. Haller, P.S. Brewster, L.D. Dworkin, C.J. Cooper, J. Tian, MicroRNA profiling in kidney disease: plasma versus plasma-derived exosomes, Gene 627 (2017) 1–8.
[128] P. Nandakumar, A. Tin, M.L. Grove, J. Ma, E. Boerwinkle, J. Coresh, A. Chakravarti, MicroRNAs in the miR-17 and miR-15 families are

downregulated in chronic kidney disease with hypertension, PLoS ONE 12 (2017) 1–13.
[129] S. Wang, Exosomal miRNAs as biomarkers in the diagnosis of liver disease, Biomark. Med. 11 (2017) 491–501.
[130] J. Chang, J.-T. Guo, D. Jiang, H. Guo, J.M. Taylor, T.M. Block, Liver-specific microRNA miR-122 enhances the replication of hepatitis C virus in nonhepatic cells, J. Virol. 82 (2008) 8215–8223.
[131] M. Girard, E. Jacquemin, A. Munnich, S. Lyonnet, A. Henrion-Caude, miR-122, a paradigm for the role of microRNAs in the liver, J. Hepatol. 48 (2008) 648–656.
[132] B. Zhou, Z. Li, H. Yang, N. He, Extracellular miRNAs: origin, function and biomarkers in hepatic diseases, J. Biomed. Nanotechnol. 10 (2014) 2865–2890.
[133] X.R. Long, Y.J. Zhang, M.Y. Zhang, K. Chen, X.F.S. Zheng, H. Yun, Identification of an 88-microRNA signature in whole blood for diagnosis of hepatocellular carcinoma and other chronic liver diseases, Aging (Albany, NY) 9 (2017) 1565–1584.
[134] C. Jin, L. Cheng, S. Höxtermann, T. Xie, X. Lu, H. Wu, A. Skaletz-Rorowski, N. Brockmeyer, N. Wu, MicroRNA-155 is a biomarker of T-cell activation and immune dysfunction in HIV-1-infected patients, HIV Med. 18 (2016) 1–9.
[135] L.P. Garo, G. Murugaiyan, Contribution of MicroRNAs to autoimmune diseases, Cell. Mol. Life Sci. 73 (2016) 2041–2051.
[136] X. Le, X. Yu, N. Shen, Novel insights of microRNAs in the development of systemic lupus erythematosus, Curr. Opin. Rheumatol. 29 (2017) 450–457.
[137] A. Mahasneh, F. Al-Shaheri, E. Jamal, Molecular biomarkers for an early diagnosis, effective treatment and prognosis of colorectal cancer: current updates, Exp. Mol. Pathol. 102 (2017) 475–483.
[138] P. Ramnani, Y. Gao, M. Ozsoz, A. Mulchandani, Electronic detection of MicroRNA at attomolar level with high specificity, Anal. Chem. 85 (2013) 8061–8064.
[139] C. Esau, S. Davis, S.F. Murray, X.X. Yu, S.K. Pandey, M. Pear, L. Watts, S.L. Booten, M. Graham, R. McKay, A. Subramaniam, S. Propp, B.A. Lollo, S. Freier, C.F. Bennett, S. Bhanot, B.P. Monia, miR-122 regulation of lipid metabolism revealed by *in vivo* antisense targeting, Cell Metab. 3 (2006) 87–98.
[140] J.M. Vargason, G. Szittya, J. Burgyán, T.M. Tanaka Hall, Size selective recognition of siRNA by an RNA silencing suppressor, Cell 115 (2003) 799–811.
[141] G. Jin, M. Cid, C.B. Poole, L.A. McReynolds, Protein mediated miRNA detection and siRNA enrichment using p19, Biotechniques 48 (2010) 17–23.
[142] H.V. Tran, B. Piro, S. Reisberg, L.D. Tran, H.T. Duc, M.C. Pham, Label-free and reagentless electrochemical detection of microRNAs using a conducting polymer nanostructured by carbon nanotubes: application to prostate cancer biomarker miR-141, Biosens. Bioelectron. 49 (2013) 164–169.
[143] H.V. Tran, B. Piro, S. Reisberg, L. Huy Nguyen, T. Dung Nguyen, H.T. Duc, M.C. Pham, An electrochemical ELISA-like immunosensor for miRNAs detection based on screen-printed gold electrodes modified with reduced graphene oxide and carbon nanotubes, Biosens. Bioelectron. 62 (2014) 25–30.
[144] F. Li, J. Peng, J. Wang, H. Tang, L. Tan, Q. Xie, S. Yao, Carbon nanotube-based label-free electrochemical biosensor for sensitive detection of miRNA-24, Biosens. Bioelectron. 54 (2014) 158–164.
[145] A.M. Cheng, M.W. Byrom, J. Shelton, L.P. Ford, Antisense inhibition of human miRNAs and indications for an involvement of miRNA in cell growth and apoptosis, Nucleic Acids Res. 33 (2005) 1290–1297.
[146] J.E. Cameron, C. Fewell, Q. Yin, J. McBride, X. Wang, Z. Lin, E.K. Flemington, Epstein-Barr virus growth/latency III program alters cellular microRNA expression, Virology 382 (2008) 257–266.
[147] F. Li, J. Peng, Q. Zheng, X. Guo, H. Tang, S. Yao, Carbon nanotube-polyamidoamine dendrimer hybrid-modified electrodes for highly sensitive electrochemical detection of microRNA24, Anal. Chem. 87 (2015) 4806–4813.
[148] L. Liu, C. Song, Z. Zhang, J. Yang, L. Zhou, X. Zhang, G. Xie, Ultrasensitive electrochemical detection of microRNA-21 combining layered nanostructure of oxidized single-walled carbon nanotubes and nanodiamonds by hybridization chain reaction, Biosens. Bioelectron. 70 (2015) 351–357.
[149] E.J. Duell, L. Lujan-barroso, N. Sala, S.D. Mcelyea, K. Overvad, A. Tjonneland, A. Olsen, E. Weiderpass, L.-T. Busund, L. Moi, D. Muller, P. Vineis, D. Aune, G. Matullo, A. Naccarati, S. Panico, G. Tagliabue, R. Tumino, D. Palli, R. Kaaks, V.A. Katze, H. Boeing, H. Bueno-de-Mesquita, P.H. Peeters, A. Trichopoulou, P. Lagiou, A. Kotanidou, R.C. Travis, N. Wareham, K.-T. Khaw, J.R. Quiros, M. Rodríguez-Barranco, M. Dorronsoro, M.-D. Chirlaque, E. Ardanaz, G. Severi, M.-C. Boutron-Ruault, V. Rebours, P. Brennan, M. Gunter, G. Scelo, G. Cote, S. Sherman, M. Korc, Plasma microRNAs as biomarkers of pancreatic cancer risk in a prospective cohort study, Int. J. Cancer 141 (2017) 905–915.
[150] W. Jinling, S. Sijing, Z. Jie, W. Guinian, Prognostic value of circulating microRNA-21 for breast cancer: a systematic review and meta-analysis, Artif. Cells Nanomed. Biotechnol. 45 (2017) 1216–1221.
[151] M. Sierzega, M. Kaczor, P. Kolodziejczyk, J. Kulig, M. Sanak, P. Richter, Evaluation of serum microRNA biomarkers for gastric cancer based on blood and tissue pools profiling: the importance of miR-21 and miR-331, Br. J. Cancer 117 (2017) 266–273.
[152] H.A. Rafiee-Pour, M. Behpour, M. Keshavarz, A novel label-free electrochemical miRNA biosensor using methylene blue as redox indicator: application to breast cancer biomarker miRNA-21, Biosens. Bioelectron. 77 (2016) 202–207.
[153] L. Wang, X. Zheng, W. Zhang, X. Quan, Q. Hu, W. Wu, P. Zong, M. Wu, One-pot synthesis of carbon-decorated FePt nanoparticles and their application for label-free electrochemical impedance sensing of DNA hybridization, RSC Adv. 3 (2013) 9042–9046.
[154] H. Fayazfar, A. Afshar, M. Dolati, A. Dolati, DNA impedance biosensor for detection of cancer, TP53 gene mutation, based on gold nanoparticles/aligned carbon nanotubes modified electrode, Anal. Chim. Acta 836 (2014) 34–44.
[155] S. Wang, L. Li, H. Jin, T. Yang, W. Bao, S. Huang, J. Wang, Electrochemical detection of hepatitis B and papilloma virus DNAs using SWCNT array coated with gold nanoparticles, Biosens. Bioelectron. 41 (2013) 205–210.
[156] A.-C. Lee, D. Du, B. Chen, C.-K. Heng, T.-M. Lim, Y. Lin, Electrochemical detection of leukemia oncogenes using enzyme-loaded carbon nanotube labels, Analyst 139 (2014) 4223–4230.
[157] A. Rafiei, A.A. Mian, C. Döring, A. Metodieva, C. Oancea, F.B. Thalheimer, M.L. Hansmann, O.G. Ottmann, M. Ruthardt, The functional interplay between the t(9;22)-associated fusion proteins BCR/ABL and ABL/BCR in Philadelphia chromosome-positive acute lymphatic leukemia, PLoS Genet. 11 (2015) 1–21.
[158] S. Singh, A. Kaushal, S. Khare, A. Kumar, mga Genosensor for early detection of human rheumatic heart disease, Appl. Biochem. Biotechnol. 173 (2014) 228–238.
[159] S. Nur Topkaya, D. Ozkan-Ariksoysal, Prostate cancer biomarker detection with carbon nanotubes modified screen printed electrodes, Electroanalysis 28 (2016) 1077–1084.
[160] M. Hasanzadeh, N. Shadjou, M. de la Guardia, Current advancement in electrochemical analysis of neurotransmitters in biological fluids, TrAC – Trends Anal. Chem. 86 (2017) 107–121.
[161] E.J. Nestler, I. Creese, D.C. Cooper, F.J. White, S. Tonegawa, A.M. Graybiel, S. Tonegawa, Hard target: understanding dopaminergic neurotransmission, Cell 79 (1994) 923–926.
[162] C.B. Jacobs, M.J. Peairs, B.J. Venton, Review: Carbon nanotube based electrochemical sensors for biomolecules, Anal. Chim. Acta 662 (2010) 105–127.
[163] S. Sansuk, E. Bitziou, M.B. Joseph, J.A. Covington, M.G. Boutelle, P.R. Unwin, J.V. Macpherson, Ultrasensitive detection of dopamine using a carbon nanotube network microfluidic flow electrode, Anal. Chem. 85 (2013) 163–169.
[164] C. Yang, C.B. Jacobs, M.D. Nguyen, M. Ganesana, A.G. Zestos, I.N. Ivanov, A.A. Puretzky, C.M. Rouleau, D.B. Geohegan, B.J. Venton, Carbon nanotubes grown on metal microelectrodes for the detection of dopamine, Anal. Chem. 88 (2016) 645–652.
[165] E. Haghshenas, T. Madrakian, A. Afkhami, Electrochemically oxidized multiwalled carbon nanotube/glassy carbon electrode as a probe for simultaneous determination of dopamine and doxorubicin in biological samples, Anal. Bioanal. Chem. 408 (2016) 2577–2586.
[166] R.M. Cardoso, R.H.O. Montes, A.P. Lima, R.M. Dornellas, E. Nossol, E.M. Richter, R.A.A. Munoz, Multi-walled carbon nanotubes: size-dependent electrochemistry of phenolic compounds, Electrochim. Acta 176 (2015) 36–43.
[167] V. Datsyuk, M. Kalyva, K. Papagelis, J. Parthenios, D. Tasis, A. Siokou, I. Kallitsis, C. Galiotis, Chemical oxidation of multiwalled carbon nanotubes, Carbon 46 (2008) 833–840.
[168] A. Gutierrez, A. Gasnier, M.L. Pedano, J.M. Gonzalez-Dominguez, A. Ansón-Casaos, J. Hernandez-Ferrer, L. Galicia, M.D. Rubianes, M.T. Martínez, G.A. Rivas, Electrochemical sensor for the quantification of dopamine using glassy carbon electrodes modified with single-wall carbon nanotubes covalently functionalized with polylysine, Electroanalysis 27 (2015) 1565–1571.
[169] J. Samseya, R. Srinivasan, A. Daniel Arulraj, V.S. Vasantha, A highly sensitive and selective multiwall carbon nanotubes/Nafion/Au microarrays electrode for dopamine determination, Electroanalysis 26 (2014) 1702–1711.
[170] I. Suzuki, M. Fukuda, K. Shirakawa, H. Jiko, M. Gotoh, Carbon nanotube multi-electrode array chips for noninvasive real-time measurement of dopamine, action potentials, and postsynaptic potentials, Biosens. Bioelectron. 15 (2013) 270–275.
[171] A. Gutiérrez, E.N. Primo, M. Eguílaz, C. Parrado, M.D. Rubianes, G.A. Rivas, Quantification of neurotransmitters and metabolically related compounds at glassy carbon electrodes modified with bamboo-like carbon nanotubes dispersed in double stranded DNA, Microchem. J. 130 (2017) 40–46.
[172] B. Zhang, D. Huang, X. Xu, G. Alemu, Y. Zhang, F. Zhan, Y. Shen, M. Wang, Simultaneous electrochemical determination of ascorbic acid, dopamine and uric acid with helical carbon nanotubes, Electrochim. Acta 91 (2013) 261–266.
[173] L.C. Recco, B.P. Crulhas, P.R.L.L. Parra, V.A. Pedrosa, A new strategy for detecting dopamine in human serum using polymer brushes reinforced with carbon nanotubes, RSC Adv. 6 (2016) 47134–47137.
[174] G. Xu, B. Li, X.T. Cui, L. Ling, X. Luo, Electrodeposited conducting polymer PEDOT doped with pure carbon nanotubes for the detection of dopamine in the presence of ascorbic acid, Sens. Actuators B: Chem. 188 (2013) 405–410.
[175] J. Liu, J. Luo, R. Liu, J. Jiang, X. Liu, Micelle-encapsulated multi-wall carbon nanotubes with photosensitive copolymer and its application in the detection of dopamine, Colloid. Polym. Sci. 292 (2014) 153–161.
[176] L. Jin, X. Gao, L. Wang, Q. Wu, Z. Chen, X. Lin, Electrochemical activation of polyethyleneimine-wrapped carbon nanotubes/*in situ* formed gold

nanoparticles functionalised nanocomposite sensor for high sensitive and selective determination of dopamine, J. Electroanal. Chem. 692 (2013) 1–8.
[177] A. Joshi, S.N. Chavan, D. Mandal, T.C. Nagaiah, Ionic liquid and nitrogen doped carbon nanotubes composite material for sensitive and selective detection of dopamine, Electroanalysis 28 (2016) 2373–2381.
[178] M. Wang, Y. Gao, J. Zhang, J. Zhao, Highly dispersed carbon nanotube in new ionic liquid-graphene oxides aqueous dispersions for ultrasensitive dopamine detection, Electrochim. Acta 155 (2015) 236–243.
[179] T. Qian, C. Yu, X. Zhou, P. Ma, S. Wu, L. Xu, J. Shen, Ultrasensitive dopamine sensor based on novel molecularly imprinted polypyrrole coated carbon nanotubes, Biosens. Bioelectron. 58 (2014) 237–241.
[180] Y. Li, J. Liu, M. Liu, F. Yu, L. Zhang, H. Tang, B.C. Ye, L. Lai, Fabrication of ultra-sensitive and selective dopamine electrochemical sensor based on molecularly imprinted polymer modified graphene@carbon nanotube foam, Electrochem. Commun. 64 (2016) 42–45.
[181] K. Jackowska, P. Krysinski, New trends in the electrochemical sensing of dopamine, Anal. Bioanal. Chem. 405 (2013) 3753–3771.
[182] E. Canbay, E. Akyilmaz, Design of a multiwalled carbon nanotube-Nafion-cysteamine modified tyrosinase biosensor and its adaptation of dopamine determination, Anal. Biochem. 444 (2014) 8–15.
[183] M.R. Bujduveanu, W. Yao, A. LeGoff, K. Gorgy, D. Shan, G.W. Diao, E.M. Ungureanu, S. Cosnier, Multiwalled carbon nanotube-$CaCO_3$ nanoparticle composites for the construction of a tyrosinase-based amperometric dopamine biosensor, Electroanalysis 25 (2013) 613–619.